CHEMISTRY
A EUROPEAN JOURNAL

DOI: 10.1002/chem.200701315

Switchable *C*- and *N*-Bound Isomers of Transition-Metal Cyanocarbanions: Synthesis and Interconversions of Cyclopentadienyl Ruthenium Complexes of Phenylsulfonylacetonitrile Anions

Takeshi Naota,* Akio Tannna, Shigeaki Kamuro, Masayuki Hieda, Kazuki Ogata, Shun-Ichi Murahashi, and Hikaru Takaya[a]

Abstract: The synthesis, structure, and dynamic behavior of bistable *C*- and *N*-bound isomers of transition-metal cyanocarbanions are described. A series of *C*-bound cyclopentadienyl (Cp) ruthenium phosphane complexes, [Ru{CH(CN)SO_2Ph}(Cp)L_1L_2] (**3**), and their *N*-bound isomers, [Ru$^+$(Cp)(NCCH$^-$$SO_2$Ph)$L_1L_2$] (**4**), were prepared by treating [RuCl(Cp)$(PR_3)_2$] with the sodium salt of phenylsulfonylacetonitrile and performing ligand-exchange reactions with the resulting compounds. Structural characterization by X-ray diffraction indicates that the cyanocarbanion moiety of **3** has an α-metalated structure, whereas that of **4** has a zwitterionic, end-on structure. Heating these complexes in aprotic solvents gives rise to irreversible linkage isomerization between *C*- and *N*-bound isomers, in which the relative thermal stabilities vary greatly depending on the steric and electronic nature of the ligands. Mechanistic studies of *N*-to-*C* isomerization revealed that the reaction proceeds irreversibly in a unimolecular manner without the formation of coordinatively unsaturated species. A metal-sliding process, which occurs over the −C−C≡N π-conjugated surface of the cyanocarbanion moiety, was suggested by results from kinetic studies and density functional theory (DFT) calculations. *C*-to-*N* isomerizations proceed by the above-mentioned intramolecular process, with a temperature-dependent contribution from the formation and cleavage of μ^2-*C*,*N* coordination dimers [{Ru{CH(CN)SO_2Ph}(Cp)-(PPh_3)}$_2$] (**15** and **16**).

Keywords: carbanions · linkage isomerization · nitriles · ruthenium · self-assembly

Introduction

The *C*-[1–4] and *N*-bound[5–7] coordination modes of transition-metal cyanocarbanions **1** and **2** have been extensively studied with respect to their molecular structure,[1,2,5] their use as reagents and catalysts for C−C bond formation,[3,4,6,8–14] and their potential use as molecular devices.[7] Most of the complexes reported are in the *C*-bound coordination mode[1,2] and can be prepared by ionic ligand exchange,[1a–d,2,3] oxidative addition to acetonitrile[1i,j] or α-halonitriles,[1e–h] or insertion into acrylonitrile.[1k,l] Complexes **1** are widely used as Grignard-type anionic reagents for selective nucleophilic addition reactions of carbonyl compounds and enones owing to their specific soft nucleophilicity.[2] Complexes **2** can be isolated, in most cases, by using a similar synthetic methodology to *C*-bound complexes[5–7] and also by C≡N bond cleavage,[5h] when they have strong electron-withdrawing groups at the α-position of the nitrile. The magnetic properties of *N*-bound complexes **2** with extended π-conjugated systems, which are potential new motifs for functional materials, have been studied extensively.[7]

The reactivity of complexes **1** and **2** has recently become a focus of interest for organic and organometallic chemists because these species have specific catalytic activity, with high selectivity and sustainability, for a variety of C−C

1 **2**

[a] Prof. Dr. T. Naota, Dr. A. Tannna, S. Kamuro, M. Hieda, K. Ogata, Prof. Dr. S.-I. Murahashi, Dr. H. Takaya
Department of Chemistry
Graduate School of Engineering Science
Osaka University
Machikaneyama, Toyonaka
Osaka 560-8531 (Japan)
Fax: (+81) 6-6850-6224
E-mail: naota@chem.es.osaka-u.ac.jp

bond-forming reactions between nitriles and electrophiles, which include carbonyl compounds,[6a–d,g,11] imines,[6b,12] nitriles,[13] electron-deficient olefins,[6b–g,11a,b,14] methylenecyclopropanes,[8] enynes,[9] allenes,[10] and bromobenzenes.[1d] Reductive elimination of **1** followed by a redox catalytic cycle has been postulated for palladium-catalyzed reactions,[1d,8–10] whereas direct nucleophilic attack on electrophiles by **2** and a nonredox mechanism occur for aldol and Michael-type reactions.[6,11]

Understanding these differences in the reactivities and properties of **1** and **2** would not only provide significant information about C–H activation and catalyzed C–C bond-formation in nitriles, but could also contribute to the design of molecular devices that are highly sensitive to stimuli. However, despite the high profile of both isomers in many fields of chemistry, the stability and dynamic behavior of these isomers is poorly understood relative to that of transition-metal enolates.[15,16] This discrepancy is probably a result of the very high stability of the C–M and M–N bonds in **1** and **2**, respectively, which mainly arises from the α-functionality of the nitrile moieties.

To obtain insight into the dynamism of **1** and **2**, we attempted to synthesize transition-metal cyanocarbanions with unprecedented stability for both *C*- and *N*-coordination modes. Sulfonyl groups, which are electron-withdrawing, but have less resonance effect, were introduced at the α-position of the coordinated nitrile moieties, thus enabling us to prepare both isomers in a stable form. This basic research led us to conduct a systematic study of the structure and properties of *C*- and *N*-bound transition-metal cyanocarbanions. A series of *C*- and *N*-bound cyclopentadienyl (Cp) ruthenium complexes of phenylsulfonylacetonitrile, anionic phosphane, and π-acidic ligands **3** and **4** ([Ru{CH(CN)SO_2Ph}(Cp)L_1L_2] and [Ru^+(Cp)(NCCH^-SO_2Ph)L_1L_2], respectively; Scheme 1) have been isolated and characterized.[17] Upon heating in an aprotic solvent, the complexes undergo selective linkage isomerization with no degradation of the coordination situation. A systematic study of ligand effects revealed that the preferred direction for *C*-to-*N* interconversion is rigidly controlled by the steric and electric nature of the ligand. Controlled experiments, kinetic studies, and density functional theory (DFT) calculations revealed that 1) *C*-to-*N* and *N*-to-*C* isomerizations proceed by an intramolecular process that involves metal slippage over the −C−C≡N π-conjugated surface, and 2) *C*-to-*N* isomerizations proceed by temperature-dependent participation of an intermolecular process that involves self-assembly of the metal atoms.[18] Herein we describe the synthesis, characterization, and *C*-to-*N* interconversions of the phenylsulfonylacetonitrile carbanion of RuCp complexes.

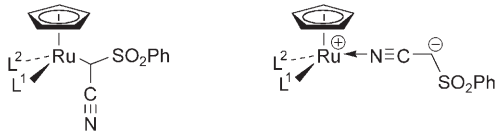

3 **4**

a: L^1 = PPh_3, L^2 = PPh_3
b: L^1 = $PMePh_2$, L^2 = $PMePh_2$
c: L^1 = PMe_2Ph, L^2 = PMe_2Ph
d: L^1 = $P(iPr)_3$, L^2 = $P(iPr)_3$
e: L^1, L^2 = $Ph_2PCH_2PPh_2$ (dppm)
f: L^1, L^2 = $Ph_2PCH_2CH_2PPh_2$ (dppe)
g: L^1, L^2 = $Ph_2P(CH_2)_4PPh_2$ (dppb)
h: L^1, L^2 = $Ph_2PCpFeCpPPh_2$ (dppf)
i: L^1, L^2 = $Me_2PCH_2CH_2PMe_2$ (dmpe)
j: L^1, L^2 = $(cC_6H_{11})_2PCH_2CH_2P(cC_6H_{11})_2$ (dcype)
k: L^1 = *t*BuNC, L^2 = PPh_3
l: L^1 = CO, L^2 = PPh_3

Scheme 1. *C*- and *N*-bound RuCp cyanocarbanions **3** and **4**.

Results and Discussion

Synthesis and characterization of *C*- and *N*-bound isomers of RuCp cyanocarbanions: A variety of *C*- and *N*-bound cyclopentadienylruthenium(II) complexes that contain the phenylsulfonylacetonitrile anion are thermally stable, and isolable through reactions of the corresponding halo complexes. Typically, when a solution of [RuCl(Cp)(PPh_3)$_2$] (**7**) was treated with Na[CH(CN)SO_2Ph] in ethanol/hexane (1:1) at RT, the isomeric mixture of the corresponding *C*- and *N*-bound PPh_3 complexes, [Ru{CH(CN)SO_2Ph}(Cp)(PPh_3)$_2$] (**3a**) and [Ru^+(Cp)(NCCH^-SO_2Ph)(PPh_3)$_2$] (**4a**), were formed in a ratio of 41:59, in which pure complex **3a** was isolated by filtration of the precipitate (37%; Scheme 2). Complex **4a** (89%) was isolated as the sole

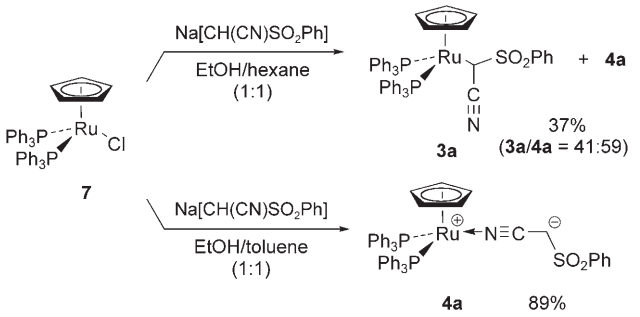

Scheme 2. Synthesis of **3a** and **4a**.

product after similar treatment in ethanol/toluene (1:1) instead of ethanol/hexane. Treating [Ru(*t*BuNC)Cl(Cp)(PPh_3)] (**8**) with Na[CH(CN)SO_2Ph] in boiling ethanol afforded the corresponding *C*-bound complex [Ru(*t*BuNC){CH(CN)-SO_2Ph}(Cp)(PPh_3)] (**3k**; 77%) as a diastereomeric mixture (65:35). A isomeric mixture (44:56) of the corresponding *C*- and *N*-bound isonitrile complexes was formed by the same reaction in ethanol/benzene (1:1) at RT, which gave the *N*-bound isomer [Ru^+(*t*BuNC)(Cp)(NCCH^-SO_2Ph)(PPh_3)] (**4k**; 18%). Similarly, the CO complexes [Ru-{CH(CN)SO_2Ph}(CO)(Cp)(PPh_3)] (**3l**; 45%, diastereomeric ratio d.r. = 91:9) and [Ru^+(CO)(Cp)(NCCH^-SO_2Ph)(PPh_3)]

(**4l**; 30%) were formed by reaction of [RuCl(CO)(Cp)-(PPh_3)$_2$] (**9**) in boiling ethanol. This is the first example, to the best of our knowledge, of the preparation of *C*- and *N*-bound isomers of transition-metal cyanocarbanions. As previously reported,[17] the second *C*- and *N*-bound isomers to be isolated were PdTp (Tp = hydrotris(pyrazolyl)borate ligand) complexes of the malononitrile anion.[2e] In contrast with the stability of both the *C*- and *N*-bound complexes of the phenylsulfonylacetonitrile anion, alkyl cyanoacetate anions coordinate exclusively in a *N*-bound manner as a result of their strong resonance effect. Typically, treating **7** with Na[CH(CN)CO_2Et] gave [Ru^+(Cp)(NCCHCO_2Et)-(PPh_3)$_2$] (**6a**) (*E*/*Z* 76:24; 70%)[6d] as the sole product.

A series of *C*- and *N*-bound phosphane complexes can be derived from **3a** and **4a** by ligand-exchange reactions with various mono- and bidentate phosphanes. Reaction of **3a** with PMe_2Ph, $Ph_2PCH_2PPh_2$ (dppm), $Ph_2PCH_2CH_2PPh_2$ (dppe), and $Me_2PCH_2CH_2PMe_2$ (dmpe) in boiling benzene gave the corresponding *C*-bound complexes [Ru{CH(CN)-SO_2Ph}(Cp)(PMe_2Ph)$_2$] (**3c**; 99%), [Ru{CH(CN)SO_2Ph}-(Cp)(dppm)] (**3e**; 73%), [Ru{CH(CN)SO_2Ph}(Cp)(dppe)] (**3f**; 73%), and [Ru(Cp){CH(CN)SO_2Ph}(dmpe)] (**3i**; 90%). Similar treatment of **4a** with $PMePh_2$, P(*i*Pr)$_3$, dppm, Ph_2P-(CH_2)$_4$$PPh_2$ (dppb), $Ph_2PCpFeCpPPh_2$ (dppf), and (cC_6H_{11})$_2$$PCH_2CH_2P$($cC_6H_{11}$)$_2$ (dcype) afforded the *N*-bound complexes [Ru^+(Cp)(NCCH^-SO_2Ph)($PMePh_2$)$_2$] (**4b**; 51%), [Ru^+(Cp)(NCCH^-SO_2Ph){P(*i*Pr)$_3$}$_2$] (**4d**; 36%), [Ru^+(Cp)-(dppm)(NCCH^-SO_2Ph)] (**4e**; 30%), [Ru^+(Cp)(dppb)-(NCCH^-SO_2Ph)] (**4g**; 85%), [Ru^+(Cp)(dppf)(NCCH^--SO_2Ph)] (**4h**; 51%), and [Ru^+(Cp)(dcype)(NCCH^-SO_2Ph)] (**4j**; 61%).

Table 1 shows selected IR and NMR spectroscopic data for **3** and **4**. CN and SO stretching bands of *C*-bound complexes **3** appear in the range of $\tilde{\nu}$ = 2189–2209 (CN), 1304–1311 (SO, asym), and 1141–1146 cm^{-1} (SO, sym), all of which are shifted to a lower frequency than those of phenylsulfonylacetonitrile ($\tilde{\nu}$ = 2258, 1318, and 1152 cm^{-1}) as a result of positive inductive effect of the metal moieties. Further shifts to lower frequency were observed for both CN ($\tilde{\nu}$ = 2163–2174 cm^{-1}) and SO ($\tilde{\nu}_{asym}$ = 1286–1305, $\tilde{\nu}_{sym}$ = 1124–1130 cm^{-1}) stretching bands of a series of complexes **4**, as a result of the strong inductive and resonance effects that arise from their naked anionic structures. σ-Donating and π-acidic ligands were found to lessen the shifts to lower frequencies mentioned above; this can be clearly seen by comparing the wavenumber obtained for **4a** ($\tilde{\nu}$ = 2163 cm^{-1}) with **4j**, **4k**, and **4l** ($\tilde{\nu}$ =, 2174, 2168, and 2172 cm^{-1}, respectively).

The chemical shifts of the C*H*CN protons in the ^{1}H NMR spectra are significantly altered by the nature of ligands in both *C*- and *N*-bound complexes. The doublet of doublet, C*H*CN proton signals of **3** in [D_6]benzene appeared between δ = 2.88 and 3.96 ppm in the following order: **3a** > **3e** > **3b** ≫ **3f** > **3k** > **3c** ≫ **3i**. Although this tendency could arise from the σ-donating properties of the ligands owing to their respective basicity (PPh_3 > $PMePh_2$ > PMe_2Ph/dppe > dmpe), the difference between the two diastereomers of **3k** (δ = 3.20 and 3.28 ppm) and the large chemical shift in **3e** cannot be explained by this inward electronic effect from the metal center. All significant variation in the C*H*CN chemical shifts of complexes **3** can be rationalized by an outward, deshielding effect from the closest benzene ring of the ligands. The C*H*CN signals of *N*-bound complexes **4** appear as a singlet between δ = 3.05 and 4.11 ppm. The size order of the chemical shifts, starting with **4b** (δ = 4.11 ppm), is **4b** > **4a**/**4j** > **4g**, are almost reversed compared with that for **3**, which suggests that the C*H*CN protons in **4** are affected by a remote, shielding effect from a specific benzene ring of the ligands.

The signals for the nitrile carbon (C*C*N) appear in the ^{13}C NMR spectra between δ = 123.6 and 126.0 ppm for **3** and δ = 151.7–154.0 ppm for **4**. The assignments of the C*C*N and *C*CN signals were confirmed by 500 MHz HMBC and HMQC NMR spectroscopy experiments, which revealed a strong correlation between the C*C*N, *C*CN, and C*H*CN signals in these complexes. Figure 1 shows that the signals from the *C*CN atom are distributed over a wide range for **3** (δ = 27.7–58.0 ppm) and a narrow range for **4** (δ = 44.0–46.3 ppm); complexes with strong σ-donating ligands tend to have signals with a higher magnetic field in both cases. These results indicate that the electronic state of *C*CN can be controlled by the electronic nature of the ligands. In particular, remote control of **4**, three atoms distant from the *C*CN atom, would provide significant information about catalytic C–C bond-forming reactions between nitriles and electro-

Table 1. Selected characterization data for ruthenium cyanocarbanions **3** and **4**.

	L_1	L_2	IR[a] [cm^{-1}]			^{1}H NMR[b] δ [ppm]	^{13}C NMR[b] δ [ppm]	
			$\tilde{\nu}$(CN)	$\tilde{\nu}_{as}$(S=O)	$\tilde{\nu}_{s}$(S=O)	C*H*CN	*C*HCN	CH*C*N
3a	PPh_3	PPh_3	2201	1304	1141	3.96	58.0	125.9
3b	$PMePh_2$	$PMePh_2$	2189	1311	1143	3.81	28.8	126.0
3c	PMe_2Ph	PMe_2Ph	2189	1310	1142	3.18	30.0	125.4
3e	$Ph_2PCH_2PPh_2$		2193	1302	1143	3.87	52.9	125.2
3f	$Ph_2P(CH_2)_2PPh_2$		2193	1304	1141	3.35	29.0	125.4
3i	$Me_2P(CH_2)_2PMe_2$		2195	1304	1144	2.88	27.7	125.5
3k	*t*BuNC	PPh_3	2201	1304	1144	3.20[c]/3.28[d]	31.0[c]/31.0[d]	124.06[c]/124.09[d]
3l	CO	PPh_3	2209	1310	1146	3.25[c]/3.43[d]	32.2[c]/32.1[d]	123.6[c]/123.6[d]
4a	PPh_3	PPh_3	2163	1286	1124	3.90	45.9	152.7
4e	$Ph_2PCH_2PPh_2$		2166	1294	1125	3.35	45.2	154.0
4g	$Ph_2P(CH_2)_4PPh_2$		2166	1305	1127	3.05	44.9	152.5
4h	Ph_2P(Cp)Fe(Cp)PPh_2		2166	1296	1127	4.09	45.8	152.7
4j	(c-C_6H_{11})$_2$$P(CH_2)_2P$($c$-$C_6H_{11}$)$_2$		2174	1292	1128	3.50	44.0	152.5
4k	*t*BuNC	PPh_3	2168	1287	1127	3.72	45.2	152.0
4l	CO	PPh_3	2172	1296	1130	3.70	46.3	151.7

[a] Recorded as a KBr disc. [b] Recorded in C_6D_6. [c] Major diastereomer (R^*_{Ru},S^*_C). [d] Minor diastereomer (R^*_{Ru},R^*_C).

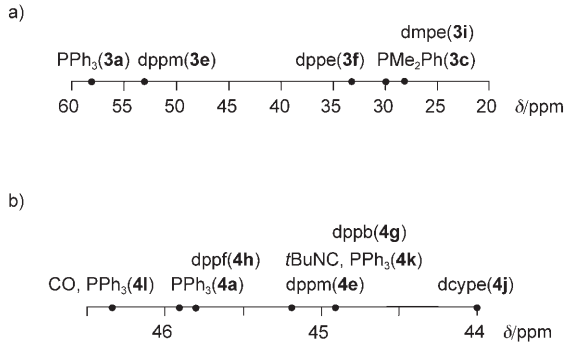

Figure 1. a) and b) Ligand dependence of ^{13}C NMR spectroscopic chemical shifts for *C*CN signals ([D_6]benzene) of **3** and **4**, respectively.

philes.[8–14] ^{31}P NMR spectra showed a pair of doublet signals for two diastereomeric P nuclei in **3**, and singlet signals in **4**.

Molecular structures of *C*- and *N*-bound complexes: The structures of the complexes were confirmed by single-crystal X-ray diffraction (Figure 2a–e shows complexes **3e**, **3k**, **3l**, **4a**, and **4k**, respectively). The crystallographic data for these complexes are listed in Table 2. Table 3 summarizes selected bond lengths and angles for these complexes and a reference nitrile (2-phenylsulfonylbutane nitrile; **10**). The bond lengths of the C≡N bonds in complexes **3** are shorter than those in **10** and increase from **3l**/**3k** > **3e**. A significant influence of the metal on the bond energies of the C≡N bonds was also demonstrated by the relative positions of the C≡N stretching bands (**10** > **3l** > **3k** > **3e**; $\tilde{\nu}$ = 2233, 2209, 2201, 2193 cm^{-1}, respectively). The Ru(1)−C(2) distances (2.166(8)–2.174(2) Å) are in the same range as the C−M bond lengths of various *C*-bound acetonitrile complexes (2.1–2.2 Å).[1–3] The bond angles of N(1)-C(1)-C(2) (177.8(6)–178.8(9)°) and the angles around the C(2) atoms indicate that the C(2) atom has high sp^3 character. These results show that complexes **3** have an almost completely α-metalated nitrile structure, in which η^2- and η^3-coordination of the metal has an almost negligible contribution.

In **4a** and **4k**, the bond angles of Ru(1)-N(1)-C(1) (172.0(4), 168.8(10)°) and N(1)-C(1)-C(2) (175.9(5), 179(1)°) demonstrate that the cyanocarbanion moieties are linear. The bond angles of C(1)-C(2)-S(1) (122.6(4), 119.3(8)°) indicate the high sp^2 character of the C(2) carbons. Complexes

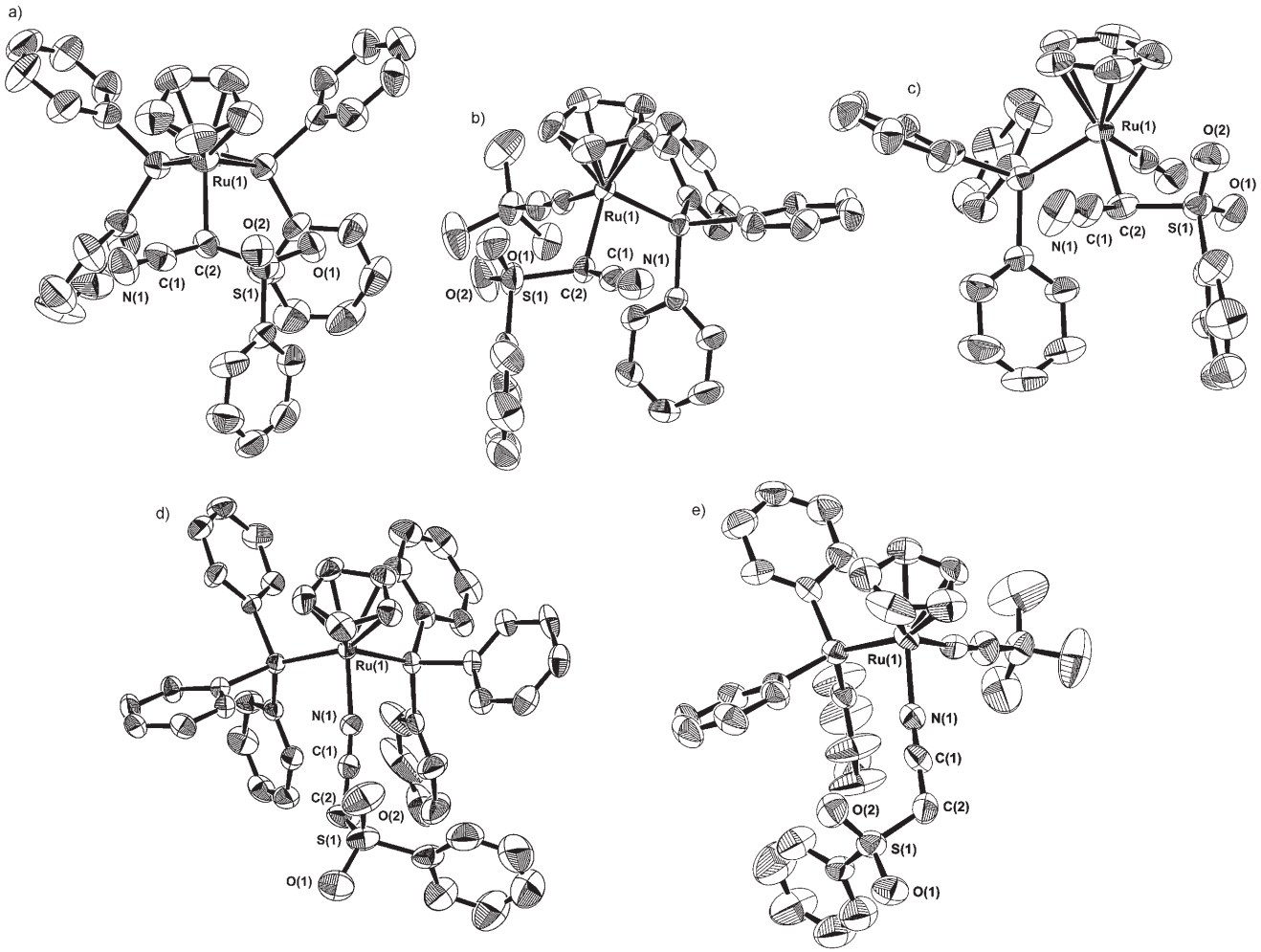

Figure 2. a)–e) Molecular structures of **3e**, **3k**, **3l**, **4a**, and **4k**, respectively.

Table 2. Crystallographic data.

	3e·$^1/_2$ CH_3COCH_3	**3k**	**3l**·C_6H_6	**4a**	**4k**·C_6H_6	**10**	**15**·C_4H_8O
formula	$C_{38}H_{33}NO_2P_2RuS$	$C_{36}H_{35}N_2O_2PRuS$	$C_{32}H_{26}NO_3PRuS$	$C_{49}H_{41}NO_2P_2RuS$	$C_{42}H_{41}N_2O_2PRuS$	$C_{10}H_{11}N_2S$	$C_{62}H_{52}N_2O_4S_2P_2Ru_2$
M_w [g mol^{-1}]	770.78	691.79	714.78	870.95	769.90	209.26	1289.41
crystal system	orthorhombic	triclinic	triclinic	monoclinic	orthorhombic	monoclinic	monoclinic
space group	*Pbca*(#61)	$P\bar{1}$(#2)	$P\bar{1}$(#2)	$P2_1/n$(#14)	$P2_12_12_1$(#19)	$P2_1/a$(#14)	C2/2(#15)
a [Å]	42.40(1)	12.769(11)	12.618(4)	10.298(2)	17.95(1)	10.900(3)	17.442(4)
b [Å]	19.648(7)	13.091(10)	13.897(8)	22.889(4)	20.169(6)	8.802(5)	16.626(9)
c [Å]	17.943(8)	11.292(6)	10.595(4)	17.333(1)	10.467(5)	11.232(5)	21.903(5)
α [°]	90	98.67(6)	103.02(4)	90	90	90	90
β [°]	90	91.78(7)	108.21(2)	95.06(1)	90	91.10(3)	96.87(2)
γ [°]	90	61.87(4)	85.51(4)	90	90	90	90
V [Å^3]	14947.9(10)	1643.8(20)	1719.5(12)	4069.5(10)	3790(2)	1077.5(8)	6306(3)
Z	16	2	2	4	4	4	8
T [°C]	20.0	23.0	23.0	23.0	23.0	20.0	20.0
reflns. collected	17059	7883	8282	10125	4872	2614	7765
independent reflns.	17059	7542	7918	9357	4843	2480	7268
obsd. [$I>2.0\sigma(I)$]	7293	6600	7160	5300	2561	1363	5114
R[a] [$I>2.0\sigma(I)$]/all	0.084/0.213	0.0275/0.0353	0.0600/0.0643	0.041/0.125	0.041/0.105	0.055/0.122	0.040/0.067
$wR2$[b] [$I>0.0\sigma(I)$]	0.2455	0.0983	0.2168	0.127	0.181	0.178	0.165
GOF	1.005	1.015	1.008	1.00	1.04	1.02	1.05

[a] $R=\frac{\sum||F_o|-|F_c||}{\sum|F_o|}$ [b] $wR2=\left[\frac{\sum w(|F_o|^2-|F_c|^2)^2}{\sum w(F_o^2)^2}\right]^{1/2}$

Table 3. Selected bond distances [Å] and angles [°] for **3e**, **3k**, **3l**, **4a**, **4k**, and **10**.

	3e	**3k**	**3l**	**4a**	**4k**	**10**
N(1)−C(1)	1.148(14)	1.144(3)	1.144(6)	1.153(6)	1.15(1)	1.134(4)
C(1)−C(2)	1.459(13)	1.446(2)	1.435(5)	1.367(7)	1.38(2)	1.439(4)
C(2)−S(1)	1.795(8)	1.782(2)	1.788(3)	1.664(6)	1.68(1)	1.807(2)
S(1)−O(1)	1.429(6)	1.429(3)	1.439(3)	1.444(5)	1.454(8)	1.432(2)
S(1)−O(2)	1.448(6)	1.435(2)	1.438(3)	1.436(5)	1.437(9)	1.435(2)
Ru(1)−C(2)	2.166(8)	2.174(2)	2.169(4)	–	–	–
Ru(1)−N(1)	–	–	–	2.054(4)	2.056(9)	–
N(1)-C(1)-C(2)	178.8(9)	178.1(2)	177.8(6)	175.9(5)	179(1)	178.0(3)
C(1)-C(2)-S(1)	106.5(6)	108.2(2)	109.0(2)	122.6(4)	119.3(8)	109.3(2)
Ru(1)-C(2)-C(1)	108.7(6)	109.89(15)	111.9(3)	–	–	–
Ru(1)-C(2)-S(1)	114.0(4)	114.01(8)	111.92(17)	–	–	–
Ru(1)-N(1)-C(1)	–	–	–	172.0(4)	168.8(10)	–

4a and **4k** have longer N(1)−C(1) bonds (1.153(6) and 1.15(1) Å, respectively) and shorter C(1)−C(2) bonds (1.367(7) and 1.38(2) Å, respectively) than **10**. This decrease in the triple-bond character of the C≡N bonds and increase in the double-bond character of C(1)−C(2) can be attributed to delocalization of the anionic charge across the C−C≡N π-conjugated surface of the cyanocarbanions. The ultimate resonance structure of metal cyanocarbanions, the azaallenyl M−N=C=C, is not appropriate in this case because the structure requires a Ru-N(1)-C(1) bond angle of 120° and the N(1)−C(1) and C(1)−C(2) bonds to have double-bond character, as seen in germanium complexes.[19] These results indicate that *N*-bound cyanocarbanions have end-on coordination and a zwitterionic electronic state with weak delocalization of the negative charge. The slight deviation of the Ru(1)-N(1)-C(1) bond angle from 180° can be attributed to steric congestion of the ligands with a small contribution from the azaallenyl electronic state.

Charge distributions on the cyanocarbanions were estimated by using DFT calculations (B3LYP/LANL2DZ) for the *C*- and *N*-bound model complexes [Ru{CH(CN)SO_2Me}(Cp)$(PH_3)_2$] (**11**) and [Ru(Cp)(NCCHSO_2Me)$(PH_3)_2$] (**12**). As shown in Figure 3, the natural bond orbital (NBO) atomic charges of the optimized geometries of **11** and **12** (Figure 8a and c, later) showed that the C(2) and N(1) atoms of **12** are much more negatively polarized than those of **11** (**11**: −0.623, −0.345 **12**: −0.771, −0.515), whereas the Ru(1) atom of **12** is positively charged compared with **11** (**11**: −0.096, **12**: −0.0007). These data are in agreement with the suggested zwitterionic electronic state of the *N*-bound complexes and clearly illustrate the significant difference in electronic state between these two species.

Interconversions between *C*- and *N*-bound cyanocarbanions: *C*- and *N*-bound complexes of transition-metal cyanocarbanions **3** and **4** undergo specific linkage isomerization upon heating in solution. Typically, complex **3a** is quantitatively converted into **4a** when heated in benzene at 60 °C, whereas

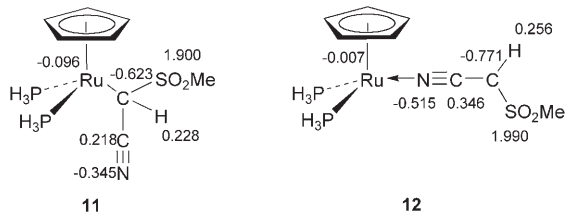

Figure 3. Selected NBO atomic charges of **11** and **12** at B3LYP/LANL2DZ (cc-pVTZ for C, H, N).

4a is thermally stable. In contrast, complex **3e** is inert to thermal isomerization, but **4e** undergoes quantitative *N*-to-*C* isomerization under similar conditions (Scheme 3). These

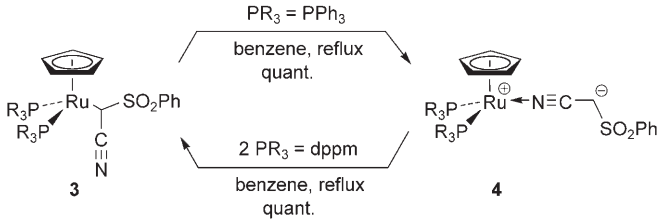

Scheme 3. *C*-to-*N* interconversions of cyanocarbanion complexes.

results indicate that the relative thermal stabilities of *C*- and *N*-bound complexes can be controlled to a large extent by the phosphane ligands. A preliminary report on these new linkage isomerizations[17] was followed by a report on a similar *N*-to-*C* isomerization in the Pd malononitrile anion [Pd(NCCHCN)MePyTp].[2e]

To pursue the ligand effect for the current linkage isomerization, we examined the thermal stability of a series of complexes **3** and **4** through ligand-exchange reactions with a number of mono- and bidentate tertiary phosphanes (Scheme 4). To identify phosphanes that induce thermal sta-

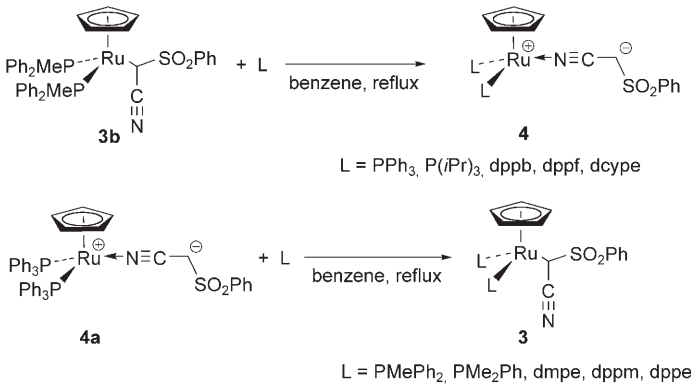

Scheme 4. Ligand-specific *C*-to-*N* interconversions.

bility in *N*-bound complexes, we investigated the reactions of thermally stable **3b** with phosphanes in boiling benzene. For **3b**, ligand exchange with particular phosphanes, which include PPh_3, $P(i\mathrm{Pr})_3$, dppb, dppf, and dcype, gave rise to subsequent quantitative isomerization to afford the corresponding *N*-bound isomers, whereas similar treatment with other phosphanes afforded the corresponding *C*-bound ones. Similarly, phosphanes that favor the *C*-bound coordination mode were found to be $PMePh_2$, PMe_2Ph, dmpe, dppm, and dppe by the ligand-exchange reaction with thermally stable **4a**.

Apparently, the σ-donating property of phosphanes is not a major controlling factor for the thermal stability of *C*- and *N*-bound complexes given its lack of correlation with the order of basicity for monodentate phosphanes ($P(i\mathrm{Pr})_3 > PMe_2Ph > PMePh_2 > PPh_3$) and for bidentate phosphanes (dmpe/dcype > dppm/dppe/dppb). However, the effects of different phosphanes correlate well with their cone angle, which is a convenient index to assess the steric situation around the metal centers of phosphane complexes.[20] As shown in Table 4, phosphanes with cone angles larger than approximately 140° stabilize the *N*-bound mode, whereas those with angles less than 140° favor the *C*-bound mode. This result shows that the relative stability of complexes **3** and **4** is mainly controlled by steric interactions between tertiary phosphanes and cyanocarbanion moieties. Such steric congestion is clearly seen in the overhead views of **3e** and **4a**, as shown in Figure 4a and c, respectively. Complex **3e** has much less steric hindrance between the bulky phenylsulfonyl group of the cyanocarbanion and the phenyl groups of dppm because of its small cone angle (Figure 4a), whereas the phenyl groups of PPh_3 in **4a** block a considerable number of regions in the cyanocarbanion moiety (Figure 4c). In other words, the dppm complex rationally selects the *C*-bound structure to obtain the original stability of the C–M bonds, rather than the zwitterionic *N*-bound coordination mode. The stable *N*-bound structure of **4a** is also preferred because it avoids energy loss from steric hindrance in the *C*-bound structure rather than gaining energy from the C–M bond.

Table 4. Correlation between the relative stability of cyanocarbanion complexes and the cone angles of their phosphane ligands.

L_1, L_2[a]	Cone angle[b] [°]	Stable structure
dmpe	107	*C* (**3i**)
dppm	121	*C* (**3e**)
PMe_2Ph	122	*C* (**3c**)
dppe	125	*C* (**3f**)
$PMePh_2$	136	*C* (**3b**)
dcype	143	*N* (**4j**)
PPh_3	145	*N* (**4a**)
dppb	145[c]	*N* (**4g**)
dppf	146[d]	*N* (**4h**)
$P(i\mathrm{Pr})_3$	160	*N* (**4d**)

[a] Abbreviations for phosphanes are as shown in Scheme 1. [b] Values are obtained from the literature unless noted otherwise.[20] [c] Estimated value based on crystallographic data for $[RuCl_2(dppb)(PPh_3)]$.[21] [d] Estimated value based on crystallographic data for $[Ru(Cp)(dppf)(C{\equiv}CC_5H_4N\{W(CO)_4(PPh_3)\})]$.[22]

N-bound complexes with π-acidic ligands, such as *t*BuNC (**4k**) and CO (**4l**), undergo facile *N*-to-*C* isomerization upon heating in boiling benzene to afford **3k** and **3l** with diastereoselectivities of 51:49 and 52:48, respectively (Scheme 5). The reaction of **4k,** in particular, proceeds smoothly even at temperatures below 60 °C, although all similar reactions with bis-phosphane ligands (Scheme 1) required overnight reflux in benzene. The ligand-exchange reaction of **4a** with *t*BuNC in boiling benzene also gave rise to quantitative formation of **3k** with the same diastereoselectivity. Complexes **3k** and **3l** do not undergo *C*-to-*N* isomerization upon heating in solution as a result of their thermal stability. As

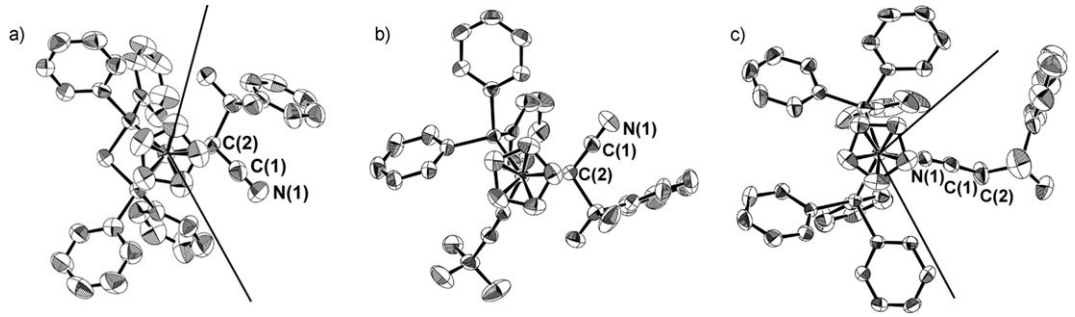

Figure 4. a)–c) Overhead views of ORTEP diagrams for **3e**, **3k**, and **4a**, respectively.

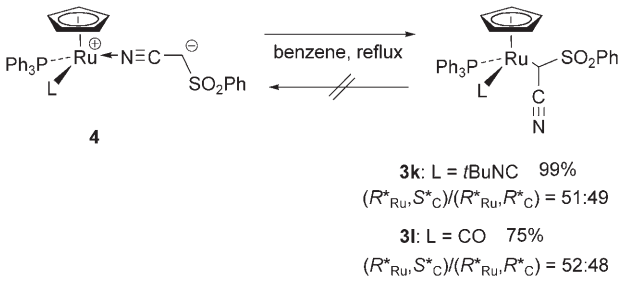

Scheme 5. Irreversible *N*-to-*C* isomerization of **4k** and **4l**.

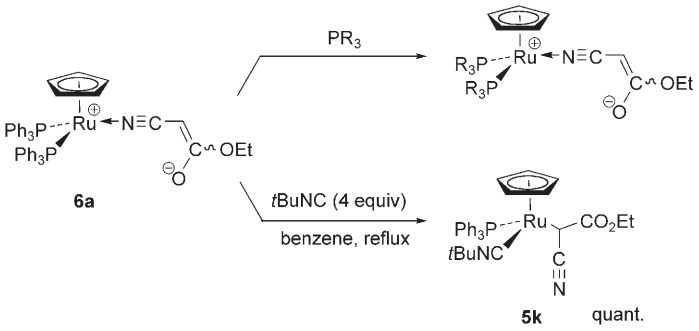

Scheme 6. *N*-to-*C* isomerization of stable cyanoacetate anion **6a**.

*t*BuNC is a less bulky ligand (as shown in the overhead view of **3k**; Figure 4b), steric effects must be a major factor in the relative thermal stabilities of **3k** and **3l**. Electronic effects that arise from the strong π acidity of the ligands would also contribute to the decrease in activation energy for η^1–η^2 transformation (conversion to side-on coordination), which is discussed later in the kinetic studies section.

Cyanocarbanion complexes that have α-CO_2R groups stabilize the zwitterionic *N*-bound coordination mode owing to a strong resonance effect in their $NCCHCO_2R$ anion moieties. Typically, the *N*-bound *bis*-PPh_3 complex $[Ru^+(Cp)(NCCHCO_2Et)(PPh_3)_2]$ (**6a**), which is highly stable as an enol,[6d] is inert with respect to *N*-to-*C* isomerization upon heating with or without any additional tertiary phosphane. Despite the high stability of *N*-bound cyanoacetate anions, addition of π-acid ligands can force the *N*-bound mode to convert into the *C*-bound mode. Reaction of **6a** with *t*BuNC (4 equiv) in boiling benzene afforded a quantitative yield of a diastereomeric mixture (d.r. = 62:38) of the corresponding *C*-bound complex, $[Ru\{CH(CN)CO_2Et\}(CNtBu)(Cp)(PPh_3)]$ (**5k**), as shown in Scheme 6. Complex **5k** can also be prepared selectively by treating $[RuCl(CNtBu)(Cp)(PPh_3)]$ (**8**) with $Na[CH(CN)CO_2Et]$ in ethanol. Note that all linkage isomerizations mentioned in this paper are irreversible, and require a reaction temperature of approximately 60 to 80 °C. No tautomerization between two coordination modes was observed under any reaction conditions.

Mechanism of *N*-to-*C* isomerization: Kinetic studies on the conversion of **4k** to **3k** in $[D_6]$benzene were carried out by means of ^1H NMR spectroscopy with dibenzyl as an internal standard.[18] Time dependence for the formation of **3k** indicated that a diastereomeric pair ((R^*_{Ru},S^*_C)-**3k** and (R^*_{Ru},R^*_C)-**3k**) was formed in a fixed ratio of 59:41 over the entire isomerization process, which shows that the process involves two independent irreversible reactions for each diastereomer. The consumption rates of **4k** exhibited clear first-order dependences ($R^2 = 1.000$ in all cases) on the concentration of **4k** at 333 to 348 K ($8.96(2)\times10^{-6}$, $1.574(7)\times10^{-5}$, $2.89(2)\times10^{-5}$, and $4.853(4)\times10^{-5}\,s^{-1}$ at 333, 338, 343, and 348 K, respectively; Figure 5), which indicates that *C*-to-*N* isomerization proceeds in a unimolecular manner. The observed first-order rate constant (k_1) fits well ($R^2 = 0.999$, Figure 6) with the Eyring relationship of $\ln(k_1/T)$ versus $1/T$, from which the activation parameters $\Delta H^{\neq}$ and $\Delta S^{\neq}$ were determined to be $(107\pm2)\,kJ\,mol^{-1}$ and $-(22\pm5)\,J\,K^{-1}\,mol^{-1}$, respectively.

Note that the rates of the isomerization of **4k** were not influenced by the solvent or additive used; the reaction in $CDCl_3$ proceeded at almost the same rate as that in $[D_6]$benzene (Table 5, entries 1 and 2). Addition of an excess of strong ligands, such as PPh_3, CH_3CN, or *t*BuNC, also had no effect on k_1 (Table 5, entries 3–5). Although a standard rationale for this reaction might involve the rate-determining formation of the 16-electron cationic complex **13** followed by a fast rebound of the counter cyanocarbanion (Scheme 7). Such a dissociation mechanism can be rejected given the above-mentioned constancy and the fact that the rate-determining formation of 16-electron complexes in ligand dissociations are significantly influenced by

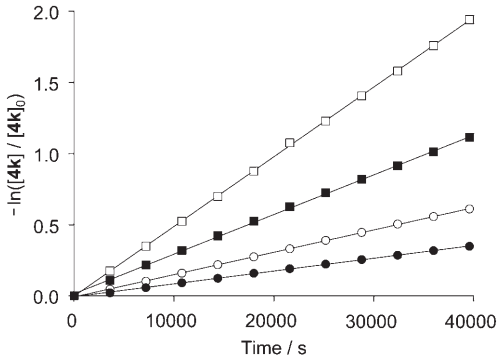

Figure 5. Time dependence of $-\ln([\mathbf{4k}]/[\mathbf{4k}]_0)$ for the isomerization of **4k** ($[\mathbf{4k}]_0 = 2.00\times10^{-2}$ M) to **3k** in [D$_6$]benzene at 333 (●), 338 (○), 343 (■), and 348 K (□).

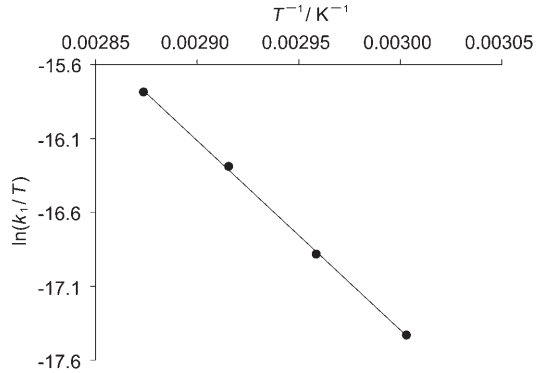

Figure 6. Eyring plot for the isomerization of **4k** ($[\mathbf{4k}]_0 = 2.00\times10^{-2}$ M) to **3k** in [D$_6$]benzene at 333–348 K. Slope $= -1.28(2)\times10^5$, intercept $=$ 21.1(6), $R^2 = 0.999$.

Table 5. First-order rate constants for the isomerization of **4k** to **3k** at 333 K.

Entry	Additive[a]	Solvent	k_1 [s^{-1}]
1	–	[D$_6$]benzene	$8.96(2)\times10^{-6}$
2	–	$CDCl_3$	$8.99(3)\times10^{-6}$
3	PPh_3	[D$_6$]benzene	$8.99(3)\times10^{-6}$
4	CH_3CN	[D$_6$]benzene	$8.67(8)\times10^{-6}$
5	*t*BuNC	[D$_6$]benzene	$8.86(9)\times10^{-6}$

[a] 4 equivalents.

the properties of solvents and external ligands.[23] Also, selective formation of **4k** with excess *t*BuNC (Table 5, entry 5) shows that the corresponding 16-electron complex [{Ru(*t*BuNC)(Cp)(PPh$_3$)}$^+$] is not formed because the same intermediate with a PF_6 counterion is known to react readily with *t*BuNC to afford [Ru(*t*BuNC)$_2$(Cp)(PPh$_3$)]PF_6.[24]

One plausible underlying mechanism for the present unimolecular reaction is a metal-sliding process, in which the metal undergoes rotation by 90° and subsequent parallel translational motion on the C–C≡N π-conjugated surface of the cyanocarbanion (Scheme 8). Linkage isomerization has

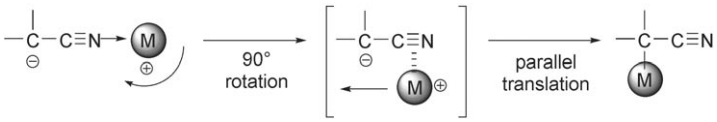

Scheme 8. Proposed metal-sliding mechanism during *N*-to-*C* isomerization.

been studied for a variety of transition-metal complexes of heteroatom compounds,[25] which includes NO,[26] NO_2,[27] SO_2,[28] Me_2SO,[28a] SCN,[28b] amides,[29] and enolates.[30] All previous cases involve a 1,2-[26–28] or 1,3-shift[28b,29,30] of the metal atom, which are reasonable movements considering the proximity of the two coordination sites on the bent ligand platforms. The mechanism proposed herein requires the metal atom to move between the considerably distant N(1) and C(2) binding sites. The most crucial step in this movement would be the initial 90° rotation, which occurs during the η^1–η^2 transformation of the nitrile coordination mode.[31] This step would be rate determining and could be accelerated by the steric and electric effects of the π-acidic ligands.

DFT calculations (B3LYP/LANL2DZ) for the transformation of **12** to **11** (Figure 3) were performed to gain insight into *C*-to-*N* linkage isomerization. Figure 7 shows a simple potential energy surface that was obtained with a sole optimized structure for transition state (TS) **14**. Optimized structures for **11**, **12**, and **14** are shown in Figure 8. TS **14** has an almost complete η^2-coordination mode as indicated by its Ru(1)-N(1)-C(1) and Ru(1)-C(1)-N(1) bond angles of 71.8 and 85.8°, respectively. Activation energy for *N*-to-*C* isomerization is estimated to be 28.3 kcal mol^{-1}, whereas that for *C*-to-*N* isomerization is 38.9 kcal mol^{-1}. This is consistent with experimental results, which show that less bulky phosphanes exclusively induce *N*-to-*C* isomerization (Table 4). The calculated reaction profile strongly supports the proposed mechanism that involves metal sliding (Scheme 8). Note that in this profile, the cyanocarbanion complex retains a noncovalent interaction between the Cp proton and the sulfonyl oxygen atom during the entire isomerization process. In other words, the flexibly rotating Cp ring acts as a hinge that supports the entropically unfavorable long-range movement of the metal. The Ru(1)-N(1)-C(1) bond angle of **12** (140.0°) shows that

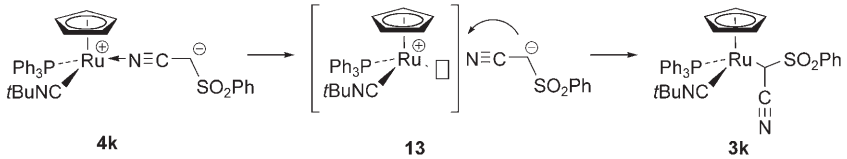

Scheme 7. Possible rate-determining step for the isomerization of **4k**, which involves the 16-electron complex **13**.

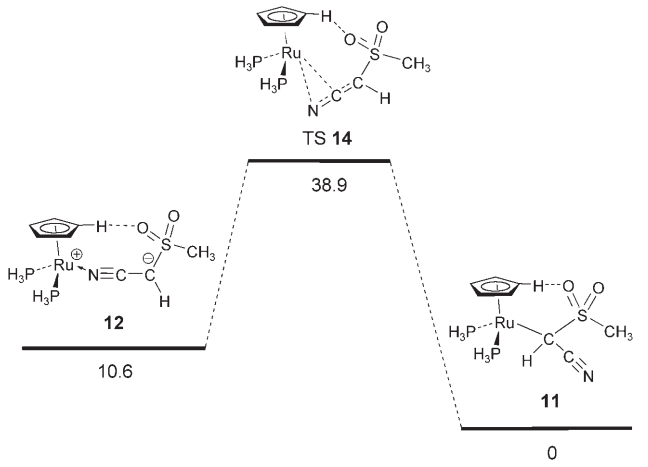

Figure 7. Potential energy profile of the isomerization of **12** to **11**. The relative free energies are given in kcal mol^{-1}.

η^1-coordination of the cyanocarbanion ligand is significantly shifted towards an azaallenyl structure to obtain this stabilization. This is in contrast with bulky complex **4a**, which has almost complete η^1-coordination with no hydrogen bonding (Figure 2). As shown in Scheme 8, the rate-determining step for this metal-sliding process is proposed to be an η^1–η^2 transformation. Therefore, this initial bending of η^1-coordination in **12** would make a significant contribution to decreasing the activation energy for this process, although this type of interaction would not generally be essential for *C*-to-*N* linkage isomerization.[2e]

Mechanism of *C*-to-*N* isomerization: *C*-to-*N* isomerization involves an alternative mechanism, which differs from the unimolecular pathway of *N*-to-*C* isomerization. As described herein, complex **3a** quantitatively afforded **4a** upon heating in boiling benzene or THF. In contrast, similar treatment of **3a** at RT in THF gave the corresponding μ^2-*C*,*N* coordination dimer[1d,32] (R^*_{Ru},S^*_C,R^*_{Ru},S^*_C)-[Ru{CH(CN)-SO_2Ph}(Cp)(PPh_3)]$_2$ (**15**) as a major product. ^{1}H NMR spectroscopic analysis of the reaction mixture indicated that **15** was formed as a single diastereomer. Analytically pure **15** (22 %) was isolated by using a reprecipitation technique and characterized by spectroscopic analyses (Scheme 9). The molecular structure of **15**, which was determined by using single-crystal X-ray diffraction (Table 2, Figure 9a), shows that the bridged cyclic structure is constructed from the strongly distorted end-on coordination of weakly bent cyano groups of *C*-bound moieties (Figure 9b). The Ru(1)-N(1)-C(1) bond angle of 156.6(3)° represents the smallest value reported to date for μ^2-*C*,*N* coordination dimers (157.8(3) and 165(5)°).[1d, 32] As expected from the distorted coordination mode, complex **15** is highly reactive with respect to ring cleavage with a variety of ligands (see Scheme 10 for examples). Treating **15** with PPh_3 and dppf in boiling benzene afforded quantitative yields of **4a** and **4h**, respectively. Similar treatment with PMe_2Ph gave rise to quantitative formation

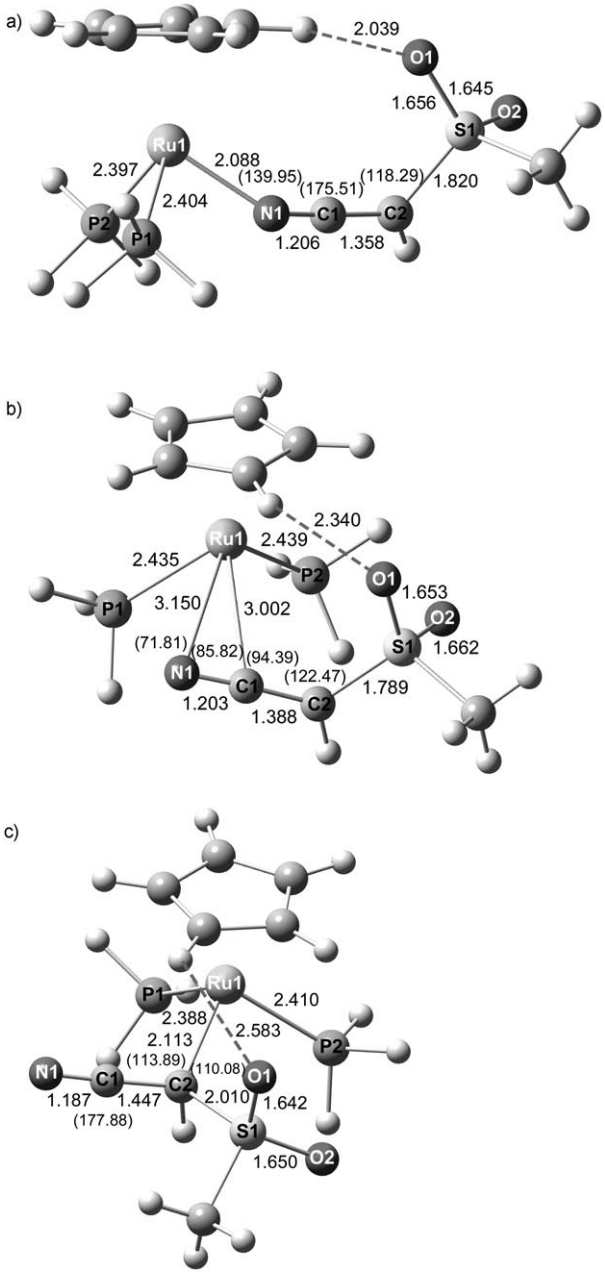

Figure 8. a)–c) Optimized geometries of **12**, TS **14**, and **11**, respectively, with selected bond lengths [Å] and angles [°].

of **3c**. Heating a solution of **15** in benzene under CO (100 atm) gave an 81:19 diastereomeric mixture of **3l**.

Changes in product distribution for the *C*-to-*N* isomerization of **3a** in [D_6]benzene between 313 and 373 K were monitored periodically by means of ^{1}H NMR spectroscopy. At 313 K, formation of a considerable amount of coordination dimer **15** and its diastereomer (**16**) was observed from the initial stage of the reaction (Figure 10a). Complex **16** was isolated and characterized by ^{1}H NMR spectroscopy in [D_6]benzene. A pair of doublet C*H*CN signals at $\delta = 4.18$ and 4.22 ppm indicated that the stereochemistry of **16** is (R^*_{Ru},R^*_C,R^*_{Ru},S^*_C) or (R^*_{Ru},R^*_C,S^*_{Ru},R^*_C) as a result its

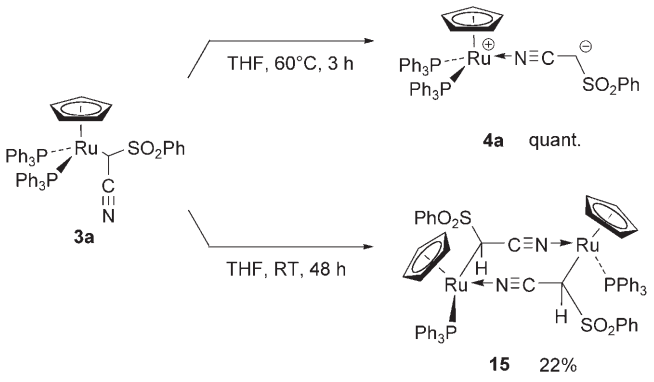

Scheme 9. The temperature-dependent reaction of **3a**.

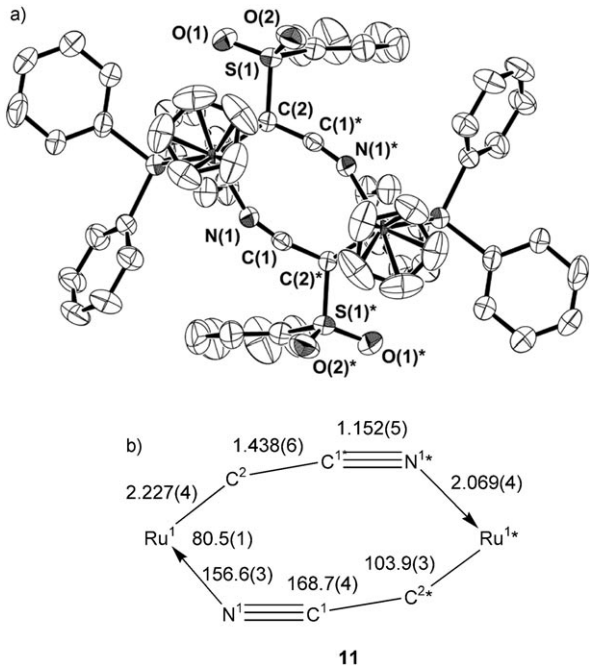

Figure 9. a) Molecular structure of **15**. b) Selected bond distances [Å] and angles [°] of **15**.

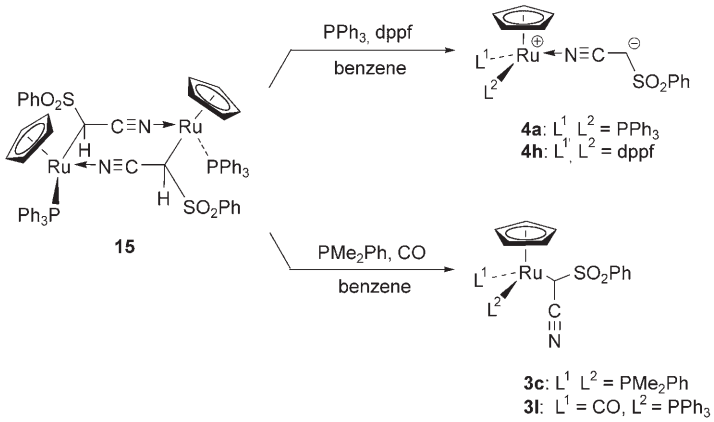

Scheme 10. Ligand-specific ring-cleavage reactions of **15**.

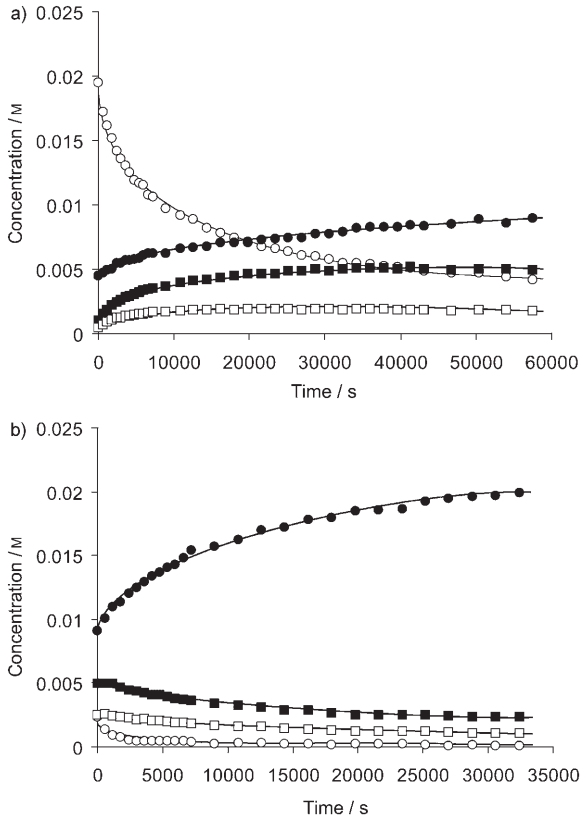

Figure 10. Reaction profiles for the isomerization of **3a** ($[\mathbf{3a}]_0 = 3.00 \times 10^{-2}$ M) to **4a** in [D$_6$]benzene at 313 (a) and 348 K (b) as evaluated by ^{1}H NMR spectroscopy. ○: **3a**, ●: **4a**, ■: **15**, □: **16**.

asymmetrical configuration. This result is in contrast with the fact that **15** was obtained exclusively with similar treatment in THF (Scheme 9). At higher temperatures, the preferential and increasing formation of **4a** was observed with slow decay of **15** and **16** (Figure 10b). In contrast, an excess of PPh_3 completely inhibited the formation of dimer intermediates. The consumption rates of **3a** exhibit clear first-order dependence ($R^2 = 0.994$–0.999) in the reaction of **3a** to **4a** PPh_3 (20 equiv) between 333 and 348 K (Figure 11), which indicates that an intramolecular direct process via a similar TS also exists in *C*-to-*N* isomerization. Activation parameters $\Delta H^{\neq}$ and $\Delta S^{\neq}$ were estimated to be (121 ± 1) and $(42 \pm 4)\,\mathrm{J\,mol^{-1}}$, respectively, from the linear Eyring relationship of $\ln(k_1/T)$ versus $1/T$ ($R^2 = 1.000$, Figure 12).

The reaction profiles in Figure 10 strongly suggest the existence of an intermolecular process in the *C*-to-*N* isomerizations, and that this process contributes strongly at higher temperatures. To investigate the putative intermolecular process, kinetic studies were carried out on the cleavage of **15** with PPh_3 (40 equiv) in [D$_6$]benzene at 313 K. The time dependence of the concentration of **3a** and **4a** showed that both complexes were formed independently without an induction period, (Figure 13) from which the initial rate constants k_{obs} ($k_{obs} = -\mathrm{d}[\mathbf{3a}]/\mathrm{d}t$, $\mathrm{d}[\mathbf{4a}]/\mathrm{d}t$) were determined to be $4.06(5) \times 10^{-8}$ and $7.00(2) \times 10^{-9}$ M s^{-1}, respectively. These k_{obs} values did not alter significantly when the reaction was car-

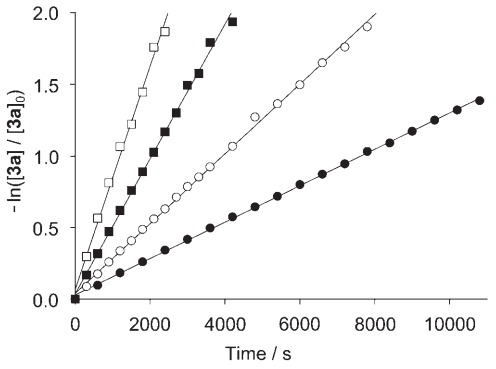

Figure 11. Time dependence of $-\ln([\mathbf{3a}]/[\mathbf{3a}]_0)$ for the isomerization of **3a** ($[\mathbf{3a}]_0 = 2.00\times10^{-2}$ M) to **4a** in the presence of PPh_3 (4.00×10^{-1} M) in [D_6]benzene, at 333 (●), 338 (○), 343 (■), and 348 K (□).

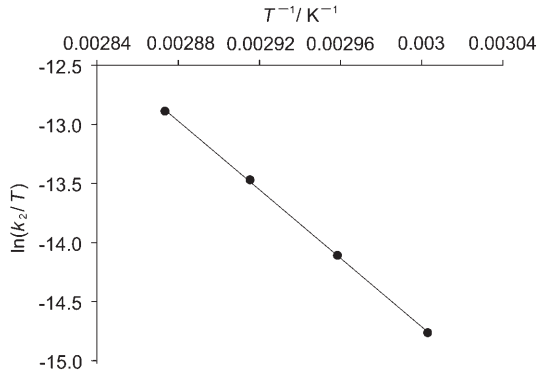

Figure 12. Eyring plot for the isomerization of **3a** ($[\mathbf{3a}]_0 = 2.00\times10^{-2}$ M) to **4a** in the presence of PPh_3 (4.00×10^{-1} M) in [D_6]benzene. Slope = $-1.45(2)\times10^4$, intercept = 28.9(5), $R^2 = 1.000$.

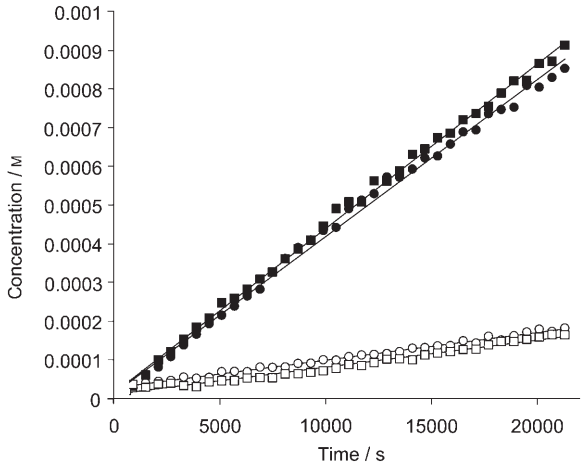

Figure 13. Time dependence of the concentrations of **3a** and **4a** for the initial reaction of **15** with PPh_3 in [D_6]benzene at 313 K, $[\mathbf{15}]_0 = 1.71\times10^{-3}$ M. ●: [**3a**], $k_{obs} = 4.06(5)\times10^{-8}$ M s^{-1}, $R^2 = 0.996$ and ○: [**4a**], $k_{obs} = 7.00(2)\times10^{-9}$ M s^{-1}, $R^2 = 0.976$ for $[PPh_3]_0 = 6.83\times10^{-2}$ M. ■: [**3a**], $k_{obs} = 4.25(3)\times10^{-8}$ M s^{-1}, $R^2 = 0.998$ and □: [**4a**], $k_{obs} = 7.16(10)\times10^{-9}$ M s^{-1}, $R^2 = 0.994$ for $[PPh_3]_0 = 1.06\times10^{-1}$ M. Data were obtained in the range of 2.9 to 13.2% conversion of **15**.

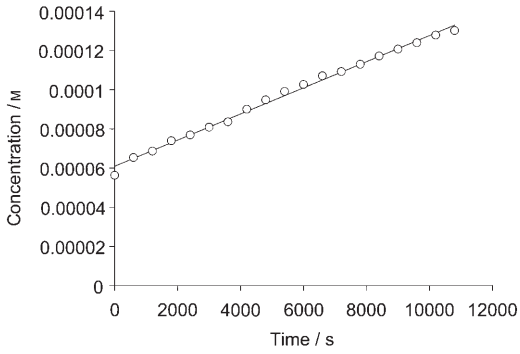

Figure 14. Time dependence of the concentration of **4a** for the initial reaction of **3a** in the presence of PPh_3 in [D_6]benzene at 313 K ($[\mathbf{3a}]_0 = 1.71\times10^{-3}$ M, $[PPh_3]_0 = 6.83\times10^{-2}$ M, $k_{obs} = 6.68(12)\times10^{-9}$ M s^{-1}, $R^2 = 0.994$). Data were obtained in the range of 3.8 to 9.4% conversion of **3a**.

ried out with different concentrations of PPh_3 (60 equiv, $k_{obs} = 4.25(3)\times10^{-8}$ and $7.16(10)\times10^{-9}$ M s^{-1} for **3a** and **4a**, respectively). These results indicate that the ring-cleavage reactions of **15** to **3a** and **4a** proceed independently by the rate-determining formation of different 16-electron complexes: [Ru{CH(CN)SO_2Ph}(Cp)(PPh_3)] for **3a** and [Ru$^+$(Cp)(NCCH$^-$$SO_2$Ph)($PPh_3$)] for **4a**.

To compare the rates of the intra- and intermolecular processes under the same reaction conditions, the value of k_{obs} for the *C*-to-*N* isomerization of **3a** with excess PPh_3 was determined under the same conditions (313 K, PPh_3, (40 equiv), Figure 14). The rate-determining step of the intramolecular process (**15** to **4a**, $k_{obs} = 7.00(2)\times10^{-9}$ M s^{-1}) was slightly faster than the intramolecular pathway (**3a** to **4a**, $k_{obs} = d[\mathbf{4a}]/dt = 6.67(12)\times10^{-9}$ M s^{-1}) in the presence of excess PPh_3 (Scheme 11). As described herein, we confirmed that the rates of isomerization of **4k** to **3k** (Table 5) and cleavage of **15** to **4a** (Figure 13) are constant with varying concentrations of PPh_3. Based on the unimolecular reaction mechanism for the direct pathway of **3a** to **4a** (Figures 11 and 12), it is reasonable to suppose that the rate for this direct pathway is also independent of PPh_3 concentration,

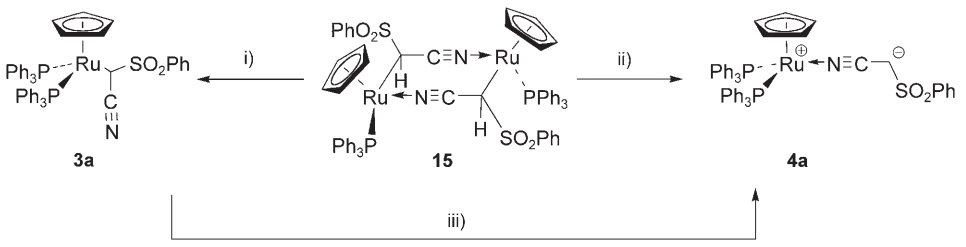

Scheme 11. i) PPh_3 (40 equiv), $k_{obs}(313\text{ K}) = 4.06(5)\times10^{-8}$ M s^{-1}. ii) PPh_3 (40 equiv), $k_{obs}(313\text{ K}) = 7.00(2)\times10^{-9}$ M s^{-1}. iii) PPh_3 (40 equiv), $k_{obs}(313\text{ K}) = 6.68(12)\times10^{-9}$ M s^{-1}.

given the postulated metal-sliding mechanism (Scheme 8). Thus we can be fairly certain that the rate for the pathway from **15** to **4a** is not negligible compared with that of the direct pathway (**3a** to **4a**), even at low concentrations of PPh_3. This conclusion implies that coordination dimers **15** and **16** are not dead-end resting states, but act as intermediates for *C*-to-*N* isomerizations.

Schematic representations of *C*-to-*N* interconversions of cyanocarbanion complexes are shown in Scheme 12. The *C*-

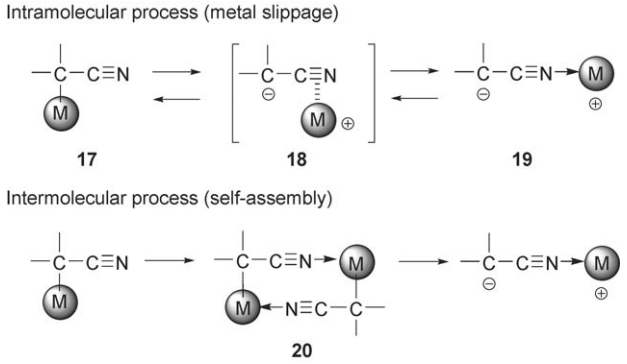

Scheme 12. Schematic representations of the *C*-to-*N* interconversions of transition-metal cyanocarbanions.

to-*N* and *N*-to-*C* transformations proceed via the same η^2-TS (**18**) in a unimolecular manner, with continuous rotational and translational motion of the metal atoms on the cyanocarbanions. Naturally, these isomerizations are postulated to proceed by η^1–η^2 transformations: **17** to **18** for *C*-to-*N*, and **19** to **18** for *N*-to-*C*. The positive $\Delta S^{\neq}$ values for the *C*-to-*N* isomerization of **3a** ($(42\pm4)\,J\,K^{-1}\,mol^{-1}$, Figure 12) can be explained by the rate-determining transformation of **17** to **18**, in which charge separation would lead to increasing randomness of the system. The negative $\Delta S^{\neq}$ values for the *N*-to-*C* isomerization of **4k** ($-(22\pm5)\,J\,K^{-1}\,mol^{-1}$, Figure 6) can be ascribed to the decreasing polarity of the zwitterionic system (**19** to **18**). Owing to the free cyano functionality of the *C*-bound complexes, the *C*-to-*N* isomerization accompanies the temperature-dependent intermolecular process, which includes the fast formation and cleavage of the corresponding μ^2-*C*,*N* coordination dimer (**20**). This is quite a rare example of a molecular transformation that is driven by self-assembly of the substrates.

Conclusion

We found that cyclopentadienyl ruthenium cyanocarbanions that have α-sulfonyl groups have unprecedented stability for both the *C*- and *N*-bound forms, and we have also succeeded in preparing exact coordination isomers of transition-metal cyanocarbanions for the first time. X-ray diffraction analyses unequivocally established that cyanocarbanions have almost complete α-metalated and end-on binding modes. Switching, irreversible linkage isomerization between the *C*- and *N*-bound isomers can be performed by heating the isomers in aprotic solvents. The direction of *C*-to-*N* interconversion, that is, the relative thermal stability of these isomers, can be controlled to a great extent by external ligands, which include mono- and bidentate phosphanes, CO, and isonitriles. Controlled experiments with regards to the reaction of thermally stable complexes **3** and **4** with various ligands revealed that the steric situation around the metal center is a major determinant of the thermal stability of these complexes. Experimental and theoretical studies on the mechanism of the *C*-to-*N* interconversions revealed that *C*-to-*N* and *N*-to-*C* isomerizations proceed by an intramolecular process and *C*-to-*N* isomerization involves a temperature-dependent intermolecular process that proceeds by the self-assembly of metal centers. *N*-Bound cyanocarbanions reportedly have high specific catalytic activity for aldol and Michael reactions, and the related carbon–carbon bond-forming reactions of nitriles.[6,8–14] These results provide interesting information regarding the controlled generation of these catalysts and a mechanistic rationale for these important catalytic processes.

Experimental Section

Preparation of 3a and 4a: A solution of $[RuCl(Cp)(PPh_3)_2]$ (**7**; 5.46 g, 7.50 mmol) and $Na[CH(CN)SO_2Ph]$ (3.05 g, 15.0 mmol) in ethanol/hexane (1:1) was stirred for 24 h at RT under an argon atmosphere. The resulting yellow precipitate was collected by filtration, washed successively with ethanol and hexane, and dried under reduced pressure to give **3a** as a yellow solid (2.41 g, 37%). Similar treatment of **7** (2.68 g, 3.70 mmol) with $Na[CH(CN)SO_2Ph]$ (1.50 g, 7.40 mmol) in ethanol/toluene (1:1) gave **4a** (2.83 g, 89%).

3a: ^1H NMR (270 MHz, C_6D_6): $\delta=3.96$ (dd, $J=8.3$, 1.7 Hz, 1H; C*H*CN), 4.90 (s, 5H; C_5H_5), 6.90–7.12 (m, 21H; Ar*H*), 7.55–7.65 (m, 12H; Ar*H*), 7.89 ppm (dd, $J=7.5$, 3.0 Hz, 2H; $SO_2C_6H_5$ (*ortho*)); $^{13}C\{^1H\}$ NMR (125 MHz, C_6D_6): $\delta=143.3$ (s; $SO_2C_6H_5$ (*ipso*)), 137.3 (s; PC_6H_5 (*ipso*)), 135.4 (d, $J=12.4$ Hz; PC_6H_5 (*ortho*)), 134.3 (d, $J=8.3$ Hz; PC_6H_5 (*meta*)), 133.9 (s; PC_6H_5 (*para*)), 131.6 (s; $SO_2C_6H_5$ (*ortho*)), 129.6 (s; $SO_2C_6H_5$ (*meta*)), 128.8 (s; $SO_2C_6H_5$ (*para*)), 125.9 (s; *C*HCN), 82.9 (s; C_5H_5), 58.0 ppm (s; *C*HCN); $^{31}P\{^1H\}$ NMR (202 MHz, C_6D_6): $\delta=42.5$ (d, $J=37.0$ Hz), 51.5 ppm (d, $J=37.0$ Hz); IR (KBr) $\tilde{\nu}=3057$, 2201 (C≡N), 1482, 1433, 1304 (asym, S=O), 1141 (sym, S=O), 1086, 745, 696 cm^{-1}; FABMS: *m*/*z*: 871 ($[M]^+$), 691 ($[Ru(Cp)(PPh_3)_2]^+$), 609 ($[Ru\{C(CN)SO_2Ph\}(Cp)(PPh_3)]^+$), 429 ($[Ru(Cp)(PPh_3)]^+$), 350, 307, 263; elemental analysis calcd (%) for $C_{49}H_{41}NO_2P_2RuS$: C 67.57, H 4.74, N 1.61; found: C 67.50, H 4.79, N 1.77.

4a: ^1H NMR (270 MHz, C_6D_6): $\delta=3.90$ (s, 1H; C*H*CN), 4.20 (s, 5H; C_5H_5), 6.94–7.08 (m, 18H; Ar*H*), 7.08–7.18 (m, 3H; Ar*H*), 7.28–7.42 (m, 12H; Ar*H*), 8.28 ppm (dd, $J=7.6$, 1.6 Hz, 2H; $SO_2C_6H_5$ (*ortho*)); $^{13}C\{^1H\}$ NMR (125 MHz, C_6D_6): $\delta=152.7$ (s; *C*HCN), 143.1 (s; $SO_2C_6H_5$ (*ipso*)), 137.6 (s; PC_6H_5 (*ipso*)), 134.0 (s; $SO_2C_6H_5$ (*ortho*)), 133.8 (s; PC_6H_5 (*ortho*)), 129.4 (s; PC_6H_5 (*meta*)), 129.1 (s; $SO_2C_6H_5$ (*meta*)), 128.8 (s; PC_6H_5 (*para*)), 128.1 (s; $SO_2C_6H_5$ (*para*)), 83.0 (s; C_5H_5), 45.9 ppm (s; *C*HCN); $^{31}P\{^1H\}$ NMR (202 MHz, C_6D_6): $\delta=42.9$ (s); IR (KBr) $\tilde{\nu}=2163$ (C≡N), 1478, 1433, 1286 (asym, S=O), 1124 (sym, S=O), 1080, 696 cm^{-1}; FABMS: *m*/*z*: 691 ($[Ru(Cp)(PPh_3)_2]^+$), 429 ($[Ru(Cp)(PPh_3)]^+$), 350; elemental analysis calcd (%) for $C_{49}H_{41}NO_2P_2RuS$: C 67.57, H 4.74, N 1.61; found: C 67.50, H 4.79, N 1.77.

Preparation of 3b: $[RuCl(Cp)(PMePh_2)_2]$ (0.151 g, 0.250 mmol) was treated with $Na[CH(CN)SO_2Ph]$ (0.102 g, 0.500 mmol) in ethanol/toluene (1:1) at RT for 72 h under an argon atmosphere. After removal of the solvent under reduced pressure, the residue was reprecipitated from ben-

zene/hexane to afford **3b** (0.015 g, 10%). ^{1}H NMR (500 MHz, C_6D_6): δ = 1.91 (d, J = 10.0 Hz, 3H; CH_3P), 2.14 (d, J = 8.0 Hz, 3H; CH_3P), 3.81 (t, J = 4.0 Hz, 1H; CHCN), 4.89 (s, 5H; C_5H_5), 6.94–7.13 (m, 15H; ArH), 7.22–7.27 (m, 4H; PC_6H_5 (*ortho*)), 7.47–7.52 (m, 4H; PC_6H_5 (*ortho*)), 8.05 ppm (dd, J = 8.0, 1.9 Hz, 2H; $SO_2C_6H_5$ (*ortho*)); ^{13}C{^{1}H} NMR (125 MHz, C_6D_6): δ = 143.9 (s; $SO_2C_6H_5$ (*ipso*)), 142.4 (d, J = 40.0 Hz; PC_6H_5 (*ipso*)), 139.8 (d, J = 38.8 Hz; PC_6H_5 (*ipso*)), 133.1 (d, J = 10.0 Hz; PC_6H_5 (*ortho*)), 132.9 (d, J = 8.8 Hz; PC_6H_5 (*ortho*)), 131.4 (d, J = 8.8 Hz; PC_6H_5 (*meta*)), 130.8 (d, J = 10.0 Hz; PC_6H_5 (*meta*)), 129.1 (s; $SO_2C_6H_5$ (*ortho*)), 129.0 (s; PC_6H_5 (*para*)), 128.9 (s; PC_6H_5 (*para*)), 128.8 (s; $SO_2C_6H_5$ (*meta*)), 128.7 (s; $SO_2C_6H_5$ (*para*)), 126.0 (dd, J = 3.2, 1.3 Hz; CHCN), 82.3 (s; C_5H_5), 28.8 (t, J = 8.8 Hz; CHCN), 19.0 (d, J = 27.5 Hz; CH$_3$P), 16.7 ppm (d, J = 27.5 Hz; CH$_3$P); ^{31}P{^{1}H} NMR (202 MHz, C_6D_6): δ = 31.5 (d, J = 39.7 Hz), 32.1 ppm (d, J = 39.7 Hz); IR (KBr) $\tilde{\nu}$ = 3053, 2980, 2916, 2189 (C≡N), 1433, 1311 (asym, S=O), 1287, 1143 (sym, S=O), 1086, 945, 911, 745, 592, 511 cm^{-1}; FABMS: m/z: 747 ([M]$^+$), 569 ([Ru(Cp)(PMePh$_2$)$_2$]$^+$), 369 ([Ru(Cp)(PMePh$_2$)]$^+$).

Preparation of 3k and 4k: [Ru(*t*BuNC)Cl(Cp)(PPh$_3$)] (**8**; 0.547 g, 1.00 mmol) was treated with Na[CH(CN)SO$_2$Ph] (0.406 g, 2.00 mmol) in boiling ethanol (40 mL) for 24 h under an argon atmosphere. Removal of the solvent and reprecipitation from benzene gave **3k** as a yellow solid (0.534 g, 77%). ^{1}H NMR spectroscopic analysis of the (Cp) groups of **3k** showed that the d.r. of (R^*_{Ru},S^*_C)-**3k**/(R^*_{Ru},R^*_C)-**3k** was 65:35. Each diastereomer was purified by recrystallization from benzene/hexane. Similar treatment of **8** (0.547 g, 1.00 mmol) with Na[CH(CN)SO$_2$Ph] (0.406 g, 2.00 mmol) in ethanol/benzene (1:1) at RT for 24 h gave **4k** as a yellow solid (0.122 g, 18%).

*(R^*_{Ru},S^*_C)-**3k***: ^{1}H NMR (500 MHz, C_6D_6): δ = 1.18 (s, 9H; C_4H_9), 3.20 (d, J = 5.0 Hz, 1H; CHCN), 5.01 (s, 5H; C_5H_5), 6.94–7.12 (m, 12H; ArH), 7.59 (dd, J = 10.5, 7.0 Hz, 6H; ArH), 8.10 ppm (d, J = 8.0 Hz, 2H; $SO_2C_6H_5$ (*ortho*)); ^{13}C{^{1}H} NMR (125 MHz, C_6D_6): δ = 144.1 (s; $SO_2C_6H_5$ (*ipso*)), 137.2 (d, J = 42.5 Hz; PC_6H_5 (*ipso*)), 134.3 (d, J = 10.5 Hz; PC_6H_5 (*ortho*)), 132.2 (s; $SO_2C_6H_5$ (*ortho*)) 131.6 (s; PC_6H_5 (*meta*)), 129.4 (s; $SO_2C_6H_5$ (*meta*)), 128.3 (s; PC_6H_5 (*para*)), 127.9 (s; $SO_2C_6H_5$ (*para*)), 124.06 (s; CHCN), 83.9 (s; C_5H_5), 56.4 (s; (CH$_3$)$_3$$C$NC), 31.0 (s; CHCN), 30.6 ppm (((CH$_3$)$_3$CNC); ^{31}P{^{1}H} NMR (202 MHz, C_6D_6): δ = 62.4 ppm (s); IR (KBr) $\tilde{\nu}$ = 2978, 2201 (C≡N), 2114 (*t*BuNC), 1480, 1433, 1304 (asym, S=O), 1211, 1144 (sym, S=O), 1092, 808, 748, 696, 590, 530 cm^{-1}; FABMS: m/z: 692 ([M]$^+$).

*(R^*_{Ru},R^*_C)-**3k***: ^{1}H NMR (500 MHz, C_6D_6): δ = 0.95 (s, 9H; C_4H_9), 3.28 (d, J = 6.5 Hz, 1H; CHCN), 5.11 (s, 5H; C_5H_5) 6.94–7.12 (m, 12H; ArH), 7.66–7.73 (m, 8H; ArH), 8.10 ppm (d, J = 8.0 Hz, 2H; $SO_2C_6H_5$ (*ortho*)); ^{13}C{^{1}H} NMR (125 MHz, C_6D_6): δ = 144.1 (s; $SO_2C_6H_5$(*ipso*)), 137.2 (d, J = 42.5 Hz; PC_6H_5 (*ipso*)), 134.3 (d, J = 10.5 Hz; PC_6H_5 (*ortho*)), 132.2 (s; $SO_2C_6H_5$ (*ortho*)) 131.6 (s; PC_6H_5 (*meta*)), 129.4 (s; $SO_2C_6H_5$ (*meta*)), 128.3 (s; PC_6H_5 (*para*)), 127.9 (s; $SO_2C_6H_5$ (*para*)), 124.09 (s; CHCN), 83.9 (s; C_5H_5), 56.4 (s; (CH$_3$)$_3$$C$NC), 31.0 (s; CHCN), 30.6 ppm (((CH$_3$)$_3$CNC); ^{31}P{^{1}H} NMR (202 MHz, C_6D_6): δ = 62.0 ppm (s).

4k: ^{1}H NMR (500 MHz, C_6D_6): δ = 0.95 (s, 9H; C_4H_9), 3.72 (s, 1H; CHCN), 4.35 (s, 5H; C_5H_5), 7.03–7.11 (m, 6H; ArH), 7.13–7.18 (m, 6H; ArH), 7.57 (dd, J = 10.5, 8.0 Hz, 6H; PC_6H_5 (*ortho*)), 8.17 ppm (dd, J = 8.0, 1.0 Hz, 2H; $SO_2C_6H_5$ (*ortho*)); ^{13}C{^{1}H} NMR (125 MHz, C_6D_6): δ = 152.6 (s; CHCN), 136.4 (d, J = 53.6 Hz; PC_6H_5 (*ipso*)), 133.9 (d, J = 13.5 Hz; PC_6H_5 (*ortho*)), 130.0 (s; PC_6H_5 (*meta*)), 129.4 (s), 128.9 (s; PC_6H_5 (*para*)), 128.6 (s), 128.5 (s), 128.5 (s), 128.2 (s), 127,8 (s), 125.8 (s; (CH$_3$)$_3$CNC), 82.2 (s; C_5H_5), 57.3 ((CH$_3$)$_3$$C$NC), 45.2 (s; CHCN), 30.6 ppm (s; (CH$_3$)$_3$CN); ^{31}P{^{1}H} NMR (202 MHz, C_6D_6): δ = 53.9 ppm (s); IR (KBr) $\tilde{\nu}$ = 2976, 2168 (C≡N), 2130 (*t*BuNC), 1480, 1433, 1287 (asym, S=O), 1256, 1208, 1127 (sym, S=O), 1094, 1078, 748, 691, 567, 530 cm^{-1}; FABMS: m/z: 692 ([M]$^+$).

Preparation of 3l and 4l: [RuCl(CO)(Cp)(PPh$_3$)] (**9**; 0.0492 g, 0.100 mmol) was treated with Na[CH(CN)SO$_2$Ph] (0.0406 g, 0.200 mmol) in boiling ethanol (4.0 mL) for 24 h under an argon atmosphere. Removal of the solvent and reprecipitation from benzene gave **3l** as a yellow solid (0.0283 g, 45%). ^{1}H NMR spectroscopic analysis of the Cp groups of **3l** showed that the d.r. of (R^*_{Ru},S^*_C)-**3l**/(R^*_{Ru},R^*_C)-**3l** was 91:9. Analytically pure (R^*_{Ru},S^*_{C*})-**3l** was obtained by recrystallization from benzene. Similar treatment of **9** (0.492 g, 1.00 mmol) with Na[CH(CN)SO$_2$Ph] (0.406 g, 2.00 mmol) in boiling ethanol (40 mL) for 6 h gave **4l** as a yellow solid (0.192 g, 30%).

*(R^*_{Ru},S^*_C)-**3l***: ^{1}H NMR (270 MHz, C_6D_6): δ = 3.25 (d, J = 7.0 Hz, 1H; CHCN), 4.96 (s, 5H; C_5H_5), 6.92–7.06 (m, 12H; ArH), 7.43–7.55 (m, 6H; ArH), 8.05 ppm (dd, J = 8.3, 1.5 Hz, 2H; $SO_2C_6H_5$ (*ortho*)); ^{13}C{^{1}H} NMR (125 MHz, C_6D_6): δ = 204.5 (s; CO), 142.4 (s; $SO_2C_6H_5$ (*ipso*)), 134.7 (d, J = 47.8 Hz; PC_6H_5 (*ipso*)), 134.0 (d, J = 11.3 Hz; PC_6H_5 (*ortho*)), 133.5 (d, J = 11.0 Hz; PC_6H_5 (*meta*)), 132.1 (s; $SO_2C_6H_5$ (*ortho*)), 130.5 (d, J = 2.4 Hz; PC_6H_5 (*para*)), 128.9 (s; $SO_2C_6H_5$ (*meta*)), 128.4 (s; $SO_2C_6H_5$ (*para*)), 123.6 (s; CHCN), 88.2 (s; C_5H_5), 32.2 ppm (CHCN); ^{31}P{^{1}H} NMR (202 MHz, C_6D_6): δ = 58.2 ppm (s); IR (KBr) $\tilde{\nu}$ = 2963, 2209 (C≡N), 1948 (CO), 1508, 1435, 1310 (asym, S=O), 1262, 1146 (sym, S=O), 1091, 1024, 802, 748, 696, 590, 530 cm^{-1}; FABMS: m/z: 636 ([M]$^+$).

*(R^*_{Ru},R^*_C)-**3l***: ^{1}H NMR (270 MHz, C_6D_6): δ = 3.43 (d, J = 4.6 Hz, 1H; CHCN), 5.01 (s, 5H; C_5H_5), 6.92–7.06 (m, 12H; ArH), 7.55–7.62 (m, 6H; ArH), 8.05 ppm (dd, J = 8.3, 1.5 Hz, 2H; $SO_2C_6H_5$ (*ortho*)); ^{13}C{^{1}H} NMR (125 MHz, C_6D_6): δ = 204.5 (s; CO), 142.4 (s; $SO_2C_6H_5$ (*ipso*)), 134.7 (d, J = 47.8 Hz; PC_6H_5 (*ipso*)), 134.0 (d, J = 11.3 Hz; PC_6H_5 (*ortho*)), 133.5 (d, J = 11.0 Hz; PC_6H_5 (*meta*)), 132.1 (s; $SO_2C_6H_5$ (*ortho*)), 130.5 (d, J = 2.4 Hz; PC_6H_5 (*para*)), 128.9 (s; $SO_2C_6H_5$ (*meta*)), 128.4 (s; $SO_2C_6H_5$ (*para*)), 123.6 (s; CHCN), 88.2 (s; C_5H_5), 32.1 (CHCN).

4l: ^{1}H NMR (500 MHz, C_6D_6): δ = 3.70 (s, 1H; CHCN), 4.41 (s, 5H; C_5H_5), 7.00–7.12 (m, 12H; ArH), 7.45–7.51 (m, 6H; ArH), 8.10 ppm (dd, J = 8.5, 1.5 Hz, 2H; $SO_2C_6H_5$ (*ortho*)); ^{13}C{^{1}H} NMR (125 MHz, C_6D_6): δ = 202.9 (d, J = 20.2 Hz; CO), 151.7 (s; CHCN), 144.1 (s; $SO_2C_6H_5$ (*ipso*)), 134.3 (d, J = 49.0 Hz; PC_6H_5 (*ipso*)), 133.6 (d, J = 11.1 Hz; PC_6H_5 (*ortho*)), 129.4 (s; PC_6H_5 (*para*)), 128.9 (d, J = 10.6 Hz; PC_6H_5 (*meta*)), 128.5 (s; $SO_2C_6H_5$ (*ortho*)), 128.3 (s; $SO_2C_6H_5$ (*meta*)), 128.3 (s; $SO_2C_6H_5$ (*para*)), 46.3 ppm (s; CHCN); ^{31}P{^{1}H} NMR (202 MHz, C_6D_6): δ = 50.0 ppm (s); IR (KBr) $\tilde{\nu}$ = 2172 (C≡N), 1960 (CO), 1480, 1435, 1296 (asym, S=O), 1260, 1130 (sym, S=O), 1096, 1080, 837, 750, 691, 610, 564, 530 cm^{-1}.

General procedure for the preparation of complexes 3 and 4 by ligand exchange reactions: The treatment of **3a** or **4a** with appropriate phosphanes was carried out in boiling benzene under an argon atmosphere. After removal of the solvent under reduced pressure, the resulting products were obtained by reprecipitation with hexane.

*Preparation and analysis of **3c***: Treating **3a** with PMe$_2$Ph (4 equiv) gave **3c** (99%). ^{1}H NMR (500 MHz, C_6D_6): δ = 1.16 (d, J = 8.5 Hz, 3H; CH_3P), 1.35 (d, J = 8.0 Hz, 3H; CH_3P), 1.41 (d, J = 9.0 Hz, 3H; CH_3P), 1.62 (d, J = 8.5 Hz, 3H; CH_3P), 3.18 (t, J = 3.5 Hz, 1H; CHCN), 4.97 (s, 5H; C_5H_5), 6.91–7.14 (m, 13H; ArH), 8.28 ppm (dd, J = 8.3, 1.5 Hz, 2H; $SO_2C_6H_5$ (*ortho*)); ^{13}C{^{1}H} NMR (125 MHz, C_6D_6): δ = 144.4 (s; $SO_2C_6H_5$ (*ipso*)), 143.1 (d, J = 39.8 Hz; PC_6H_5 (*ipso*)), 142.1 (d, J = 37.0 Hz; PC_6H_5 (*ipso*)), 131.9 (s; $SO_2C_6H_5$ (*ortho*)), 130.6 (d, J = 10.1 Hz; PC_6H_5 (*ortho*)), 129.7 (d, J = 9.1 Hz; PC_6H_5 (*ortho*)), 128.9 (s; $SO_2C_6H_5$ (*meta*)), 128.8 (s), 128.7 (d, J = 3.2 Hz; PC_6H_5 (*meta*)), 128.6 (d, J = 3.0 Hz; PC_6H_5 (*meta*)), 128.5 (s; $SO_2C_6H_5$ (*para*)), 128.3 (s), 128.1 (s; PC_6H_5 (*para*)), 127.9 (s; PC_6H_5 (*para*)), 125.4 (dd, J = 4.3, 3.4 Hz; CHCN), 81.6 (s; C_5H_5), 30.0 (dd, J = 9.6, 7.2 Hz; CHCN), 24.0 (dd, J = 29.4, 3.3 Hz; CH$_3$P), 21.2 (d, J = 29.4 Hz; CH$_3$P), 18.2 (d, J = 26.0 Hz; CH$_3$P), 15.1 ppm (d, J = 24.4 Hz; CH$_3$P); ^{31}P{^{1}H} NMR (202 MHz, C_6D_6): δ = 21.3 (d, J = 46.3 Hz), 15.1 ppm (d, J = 46.3 Hz); IR (KBr) $\tilde{\nu}$ = 3034, 3004, 2978, 2189 (C≡N), 1480, 1433, 1310 (asym, S=O), 1287, 1142 (sym, S=O), 1098, 943, 911, 831, 745, 592, 540, 494 cm^{-1}; FABMS: m/z: 623 ([M]$^+$), 485 ([Ru(Cp)(NCCHSO$_2$Ph)(PMe$_2$Ph)]$^+$), 443 ([Ru(Cp)(PMe$_2$Ph)$_2$]$^+$), 305 ([Ru(Cp)(PMe$_2$Ph)]$^+$).

*Preparation and analysis of **3e***: Treating **3a** with dppm (2 equiv) gave **3e** (73%). ^{1}H NMR (270 MHz, C_6D_6): δ = 3.87 (dd, J = 6.0, 3.2 Hz, 1H; CHCN), 4.57 (t, J = 9.8 Hz, 2H; PCH_2P), 4.93 (s, 5H; C_5H_5), 6.85–6.94 (m, 12H; ArH), 7.09–7.20 (m, 8H; ArH), 7.77 (m, 3H; ArH), 8.02 ppm (m, 2H; $SO_2C_6H_5$ (*ortho*)); ^{13}C{^{1}H} NMR (125 MHz, C_6D_6): δ = 144.7 (s; $SO_2C_6H_5$ (*ipso*)), 141.6 (dd, J = 36.5, 7.6 Hz; PC_6H_5 (*ipso*)), 138.6 (dd, J = 35.3, 8.8 Hz; PC_6H_5 (*ipso*)), 137.4 (dd, J = 27.7, 3.8 Hz; PC_6H_5 (*ipso*)), 135.6 (dd, J = 36.5, 3.8 Hz; PC_6H_5 (*ipso*)), 132.8 (t, J = 12.6 Hz; PC_6H_5 (*ortho*)), 132.4 (d, J = 10.1 Hz; PC_6H_5 (*ortho*)), 132.0 (t, J = 13.9 Hz; PC_6H_5 (*ortho*)), 131.4 (s; $SO_2C_6H_5$ (*ortho*)), 130.3 (s), 130.1 (s; PC_6H_5 (*meta*)), 130.0 (s; PC_6H_5 (*meta*)), 129.0 (s; PC_6H_5 (*para*)), 128.84 (s),

128.76 (s), 128.63 (s; $SO_2C_6H_5$ (*para*)), 128.55 (s), 128.52 (s), 128.45 (s), 127.6 (s), 125.2 (dd, $J=5.0$, 2.5 Hz; CHCN), 82.4 (s; C_5H_5), 82.3 (s; C_5H_5), 52.9 (t, $J=21.4$ Hz; *C*HCN), 29.9–30.1 ppm (m, P*C*H$_2$P); $^{31}P\{^1H\}$ NMR (202 MHz, C_6D_6): $\delta=7.82$ (d, $J=96.3$ Hz), 13.3 ppm (d, $J=96.3$ Hz); IR (KBr) $\tilde{\nu}=2193$ (C≡N), 1435, 1302 (asym, S=O), 1143 (sym, S=O), 1086, 590, 536, 511 cm^{-1}; FABMS: *m*/*z*: 730 ($[M]^+$), 589, 550 ($[Ru(Cp)(dppm)]^+$), 307; elemental analysis calcd (%) for $C_{38}H_{33}NO_2P_2RuS$: C 62.46, H 4.55, N 1.92; found: C 62.39, H 4.59, N 1.99.

Preparation and analysis of ***3f***: Treating **3a** with dppe (2 equiv) gave **3f** (73%). ^1H NMR (270 MHz, C_6D_6): $\delta=3.35$ (dd, $J=5.7$, 2.3 Hz, 1H; C*H*CN), 4.78 (s, 5H; C_5H_5), 7.03–7.16 (m, 15H; Ar*H*), 7.27–7.40 (m, 8H; PC$_6H_5$ (*ortho*)), 8.12 ppm (dd, $J=10.1$, 7.6 Hz, 2H; $SO_2C_6H_5$ (*ortho*)); $^{13}C\{^1H\}$ NMR (125 MHz, C_6D_6): $\delta=144.9$ (d, $J=42.9$ Hz; P*C*$_6H_5$ (*ipso*)), 143.8 (s; $SO_2C_6H_5$ (*ipso*)), 139.8 (d, $J=42.9$ Hz; P*C*$_6H_5$ (*ipso*)), 137.2 (d, $J=33.8$ Hz; P*C*$_6H_5$ (*ortho*)), 135.9 (d, $J=33.9$ Hz; P*C*$_6H_5$ (*ortho*)), 133.9 (d, $J=11.3$ Hz; P*C*$_6H_5$ (*meta*)), 132.3 (d, $J=10.0$ Hz; P*C*$_6H_5$ (*meta*)), 132.0 (d, $J=9.6$ Hz; P*C*$_6H_5$ (*para*)), 131.6 (s; $SO_2C_6H_5$ (*ortho*)), 130.3 (s; $SO_2C_6H_5$ (*meta*)), 130.0 (d, $J=9.6$ Hz; P*C*$_6H_5$ (*para*)), 128.6 (s; $SO_2C_6H_5$ (*para*)), 125.4 (s; CHCN), 83.5 (s; C_5H_5), 32.4 (dd, $J=30.3$, 16.6 Hz; P*C*H$_2$*C*H$_2$P), 29.0 (dd, $J=6.9$, 1.3 Hz; *C*HCN), 27.2 ppm (dd, $J=32.0$, 15.3 Hz; PCH$_2$*C*H$_2$P); $^{31}P\{^1H\}$ NMR (202 MHz, C_6D_6): $\delta=79.2$ (d, $J=64.0$ Hz), 82.3 ppm (d, $J=64.0$ Hz); IR (KBr) $\tilde{\nu}=2193$ (C≡N), 1482, 1435, 1304 (asym, S=O), 1188, 1141 (sym, S=O), 1098, 742, 694, 530 cm^{-1}; FABMS: *m*/*z*: 745 ($[M]^+$), 600, 567, 432.

Preparation and analysis of ***3i***: Treating **3a** with dmpe (2 equiv) gave **3i** (90%). ^1H NMR (500 MHz, C_6D_6): $\delta=0.60$–0.71 (m, 1H; PC*H*$_2$CH$_2$P), 0.81–1.06 (m, 2H; PC*H*$_2$CH$_2$P), 0.97 (d, $J=9.0$ Hz, 3H; PC*H*$_3$), 1.21 (d, $J=8.5$ Hz, 6H; PC*H*$_3$), 1.23 (d, $J=8.5$ Hz, 3H; PC*H*$_3$), 1.25–1.35 (m, 1H; PC*H*$_2$CH$_2$P), 2.88 (dd, $J=4.0$, 1.5 Hz, 1H; C*H*CN), 4.84 (s, 5H; C_5H_5), 7.03 (tt, $J=7.5$, 2.5 Hz, 1H; $SO_2C_6H_5$ (*para*)), 7.09 (tt, $J=8.0$, 2.0 Hz, 2H; $SO_2C_6H_5$ (*meta*)), 8.29 ppm (dd, $J=8.0$, 1.5 Hz, 2H; $SO_2C_6H_5$ (*ortho*)); $^{13}C\{^1H\}$ NMR (125 MHz, C_6D_6): $\delta=144.9$ (s; $SO_2C_6H_5$ (*ipso*)), 131.8 (s; $SO_2C_6H_5$ (*ortho*)), 128.8 (s; $SO_2C_6H_5$ (*meta*)), 127.9 (s; $SO_2C_6H_5$ (*para*)), 125.5 (t, $J=3.2$ Hz; CHCN), 80.9 (t, $J=2.4$ Hz; C_5H_5), 33.4 (dd, $J=31.8$, 18.3 Hz; P*C*H$_2$CH$_2$P), 29.5 (dd, $J=30.4$, 15.9 Hz; PCH$_2$*C*H$_2$P), 27.7 (dd, $J=8.2$, 5.8 Hz; *C*HCN), 22.1 (d, $J=27.7$ Hz; P*C*H$_3$), 20.9 (d, $J=28.5$ Hz; P*C*H$_3$), 16.9 (d, $J=20.7$ Hz; P*C*H$_3$), 15.8 ppm (d, $J=19.8$ Hz; P*C*H$_3$); $^{31}P\{^1H\}$ NMR (202 MHz, C_6D_6): $\delta=52.7$ (d, $J=34.2$ Hz), 54.1 ppm (d, $J=34.2$ Hz); IR (KBr) $\tilde{\nu}=3017$, 2928, 2907, 2195 (C≡N), 1424, 1304 (asym, S=O), 1144 (sym, S=O), 938, 733, 590 cm^{-1}; FABMS: *m*/*z*: 497 ($[M]^+$).

Preparation and analysis of ***4b***: Treating **4a** with $PMePh_2$ (6 equiv) gave **4b** (51%). ^1H NMR (500 MHz, C_6D_6): $\delta=1.40$–1.48 (br m, 6H; C*H*$_3$P), 4.11 (s, 1H; C*H*CN), 4.16 (s, 5H; C_5H_5), 6.94–7.13 (m, 15H; Ar*H*), 7.30–7.45 (m, 8H; PC$_6H_5$ (*ortho*)), 8.30 ppm (d, $J=8.0$ Hz, 2H; $SO_2C_6H_5$ (*ortho*)); $^{31}P\{^1H\}$ NMR (202 MHz, C_6D_6): $\delta=33.1$ ppm (s); IR (KBr) $\tilde{\nu}=$ 3056, 2921, 2170 (C≡N), 1480, 1435, 1267 (asym, S=O), 1140 (sym, S=O), 1128, 1096, 1078, 889, 750, 694, 590, 507 cm^{-1}; FABMS: *m*/*z*: 747 ($[M]^+$), 569 ($[Ru(Cp)(PMePh_2)_2]^+$), 369 ($[Ru(Cp)(PMePh_2)]^+$).

Preparation and analysis of ***4d***: Treating **4a** with P(*i*Pr)$_3$ (4 equiv) gave **4d** (36%). ^1H NMR (270 MHz, C_6D_6): $\delta=0.70$–1.40 (m, 42H; PC$_3H_7$), 3.39 (s, 1H; C*H*CN), 4.25 (s, 5H; C_5H_5), 6.75–7.15 (m, 3H; Ar*H*), 8.00–8.10 ppm (m, 2H; $SO_2C_6H_5$ (*ortho*)); $^{31}P\{^1H\}$ NMR (202 MHz, C_6D_6): $\delta=$ 39.7 ppm (s); IR (KBr) $\tilde{\nu}=3056$, 2961, 2924, 2170 (C≡N), 2072, 1480, 1433, 1261 (asym, S=O), 1144 (sym, S=O), 1088, 1028, 747, 696, 521 cm^{-1}.

Preparation and analysis of ***4e***: Treating **4a** with dppm (1.1 equiv) gave **4e** (30%). ^1H NMR (500 MHz, C_6D_6): $\delta=3.35$ (s, 1H; C*H*CN), 4.44 (s, 5H; C_5H_5), 4.53 (dt, $J=15.0$, 11.0 Hz, 1H; PC*H*$_2$P), 4.68 (dt, $J=15.0$, 11.0 Hz, 1H; PC*H*$_2$P), 6.86–7.16 (m, 15H; Ar*H*), 7.28–7.33 (m, 4H; PC$_6H_5$ (*ortho*)), 7.72–7.77 (m, 4H; P*C*$_6H_5$ (*ortho*)), 7.85 ppm (dd, $J=8.0$, 2.1 Hz, 2H; $SO_2C_6H_5$ (*ortho*)); $^{13}C\{^1H\}$ NMR (125 MHz, C_6D_6): $\delta=154.0$ (s; N*C*CH$^-$), 146.7 (s; $SO_2C_6H_5$ (*ipso*)), 132.8 (s; P*C*$_6H_5$ (*ipso*)), 132.3 (s; P*C*$_6H_5$ (*ortho*)), 131.7 (s; $SO_2C_6H_5$ (*ortho*)), 130.8 (s; P*C*$_6H_5$ (*meta*)), 129.9 (s; $SO_2C_6H_5$ (*meta*)), 129.7 (s; P*C*$_6H_5$ (*para*)), 128.2 (s; $SO_2C_6H_5$ (*para*)), 78.6 (s; C_5H_5), 45.2 (s; NC*C*H), 27.7 ppm (P*C*H$_2$P); $^{31}P\{^1H\}$ NMR (202 MHz, C_6D_6): $\delta=14.3$ ppm (s); IR (KBr) $\tilde{\nu}=2166$ (C≡N), 1435, 1294 (asym, S=O), 1258, 1125 (sym, S=O), 1100, 1076, 725, 513 cm^{-1}; FABMS: *m*/*z*: 731 ($[M]^+$), 551 ($[Ru(Cp)(dppm)]^+$).

Preparation and analysis of ***4g***: Treating **4a** with dppb (1.1 equiv) gave **4g** (85%). ^1H NMR (270 MHz, C_6D_6): $\delta=1.09$–1.30 (br m, 4H; C*H*$_2$CH$_2$P), 1.79–2.04 (br m, 2H; C*H*$_2$P), 2.98–3.14 (br m, 2H; C*H*$_2$P), 3.04–3.06 (br m, 1H; C*H*CN), 3.96 (s, 5H; C_5H_5), 7.06–7.18 (br m, 18H; Ar*H*), 7.38–7.47 (br m, 12H; Ar*H*), 8.231 ppm (dd, $J=8.4$, 2.0 Hz; $SO_2C_6H_5$ (*ortho*)); $^{13}C\{^1H\}$ NMR (125 MHz, C_6D_6): $\delta=152.5$ (s; CHCN), 141.9 (s; $SO_2C_6H_5$ (*ipso*)), 139.7 (s; P*C*$_6H_5$ (*ipso*)), 137.9 (s; P*C*$_6H_5$ (*ortho*)), 134.0 (s; $SO_2C_6H_5$ (*ortho*)), 132.7 (s; P*C*$_6H_5$ (*meta*)), 132.2 (s; $SO_2C_6H_5$ (*meta*)), 129.7 (s; P*C*$_6H_5$ (*para*)), 129.5 (s; $SO_2C_6H_5$ (*para*)), 81.7 (s; C_5H_5), 44.9 (s; *C*HCN), 29.3 (s; *C*H$_2$), 28.2 (s; *C*H$_2$), 23.6 (s; *C*H$_2$), 23.4 ppm (s; *C*H$_2$); $^{31}P\{^1H\}$ NMR (202 MHz, C_6D_6): $\delta=46.2$ ppm (s); IR (KBr) $\tilde{\nu}=3051$, 2166 (C≡N), 1480, 1433, 1305 (asym, S=O), 1127 (sym, S=O), 1093, 1080, 745, 696, 517 cm^{-1}; FABMS: *m*/*z*: 774 ($[M]^+$), 691, 595 ($[Ru(Cp)(dppb)]^+$).

Preparation and analysis of ***4h***: Treating **4a** with dppf (1.05 equiv) gave **4h** (51%). ^1H NMR (270 MHz, C_6D_6): $\delta=3.67$–3.73 (br m, 2H; PC$_5H_4$), 3.99 (s, 5H; C_5H_5), 4.04–4.07 (br m, 2H; P C$_5H_4$), 4.09 (s, 1H; C*H*CN), 4.15–4.18 (br m, 2H; P C$_5H_4$), 5.34–5.37 (br m, 2H; P C$_5H_4$), 7.00–7.15 (m, 12H; Ar*H*), 7.33–7.40 (br m, 4H; Ar*H*), 7.75–7.83 (br m, 4H; Ar*H*), 8.33 ppm (dd, $J=8.0$, 2.1 Hz, 2H; $SO_2C_6H_5$ (*ortho*)); $^{13}C\{^1H\}$ NMR (125 MHz, C_6D_6): $\delta=152.7$ (s; CH*C*N), 141.2 (s; $SO_2C_6H_5$ (*ipso*)), 140.7 (d, $J=33.9$ Hz; P*C*$_6H_5$ (*ipso*)), 140.5 (d, $J=35.4$ Hz; P*C*$_6H_5$ (*ipso*)), 138.8 (d, $J=37.0$ Hz; P*C*$_6H_5$ (*ipso*)), 138.6 (d, $J=38.6$ Hz; P*C*$_6H_5$ (*ipso*)), 134.4 (s), 133.5 (d, $J=23.6$ Hz; P*C*$_6H_5$ (*ortho*)), 129.9 (s; $SO_2C_6H_5$ (*ortho*)), 129.6 (s; P*C*$_6H_5$ (*meta*)), 129.2 (s; P*C*$_6H_5$ (*para*)), 128.5 (s; $SO_2C_6H_5$ (*meta*)), 128.4 (s; $SO_2C_6H_5$ (*para*)), 128.3 (s), 128.1 (s), 127.9 (s), 127.6 (s), 126.0 (s), 125.8 (s), 86.1 (d, $J=38.0$ Hz; P*C*$_5H_4$), 85.9 (d, $J=36.0$ Hz; P*C*$_5H_4$), 82.5 (s; C_5H_5), 75.9 (s; P*C*$_5H_4$), 73.5 (s; P*C*$_5H_4$), 73.4 (s; P*C*$_5H_4$), 72.9 (s; P*C*$_5H_4$), 69.3 (s; P*C*$_5H_4$), 69.1 (s; P*C*$_5H_4$), 45.8 ppm (s; *C*HCN); $^{31}P\{^1H\}$ NMR (202 MHz, C_6D_6): $\delta=49.4$ ppm (s); IR (KBr) $\tilde{\nu}=2166$ (C≡N), 1480, 1433, 1296 (asym, S=O), 1127 (sym, S=O), 1080, 747, 696, 608 cm^{-1}; FABMS: *m*/*z*: 900 ($[M]^+$), 720 ($[Ru(Cp)(dppf)]^+$), 429, 307.

Preparation and analysis of ***4j***: Treating **4a** with dcype (1.1 equiv) gave **4j** (61%). ^1H NMR (500 MHz, C_6D_6): $\delta=1.20$–1.98 (br m, 48H; $C_{12}H_{22}PC_2H_4PC_{12}H_{22}$), 3.40–3.60 (br m, 1H; C*H*CN), 4.57 (s, 5H; C_5H_5), 7.10–7.13 (m, 2H; $SO_2C_6H_5$ (*meta*)), 7.17 (t, $J=7.0$ Hz, 1H; $SO_2C_6H_5$ (*para*)), 8.26 ppm (dd, $J=10.5$, 1.5 Hz, 2H; $SO_2C_6H_5$ (*ortho*)); $^{13}C\{^1H\}$ NMR (125 MHz, C_6D_6): $\delta=152.5$ (s; CH*C*N), 134.1 (s; $SO_2C_6H_5$ (*ipso*)), 129.2 (s; $SO_2C_6H_5$ (*ortho*)), 128.5 (s; $SO_2C_6H_5$ (*meta*)), 127.6 (s; $SO_2C_6H_5$ (*para*)), 77.2 (s; C_5H_5), 44.0 (s; *C*HCN), 40.5 (dd, $J=19.2$, 15.6 Hz; P*C*H$_2$CH$_2$P), 37.1 (t, $J=19.2$ Hz; PCH$_2$*C*H$_2$P), 30.8 (s; C_6H_{11}), 29.7 (s; C_6H_{11}), 29.6 (s; C_6H_{11}), 28.1–27.9 (m, C_6H_{11}), 27.8–27.6 (m, C_6H_{11}), 27.0 (s; C_6H_{11}), 26.5 (s; C_6H_{11}), 22.1 (s; C_6H_{11}), 21.9 (s; C_6H_{11}), 21.7 ppm (s; C_6H_{11}); $^{31}P\{^1H\}$ NMR (202 MHz, C_6D_6): $\delta=88.5$ ppm (s); IR (KBr) $\tilde{\nu}=2928$, 2851, 2174 (C≡N), 1447, 1292 (asym, S=O), 1261, 1128 (asym, S=O), 1080, 1043, 891, 853, 801, 750, 691, 530 cm^{-1}; FABMS: *m*/*z*: 769 ($[M]^+$), 589 ($[Ru(Cp)(dcype)]^+$).

Isomerization of 3 to 4: The general procedure for *C*-to-*N* isomerization is exemplified by the conversion of **3a** to **4a**: A solution of **3a** (0.0109 g, 0.0125 mmol) in benzene (10.0 mL) was heated at 60 °C for 3 h under an argon atmosphere. Evaporation of the solvent under reduced pressure gave an orange residue. ^1H NMR (270 MHz, C_6D_6) spectroscopic analysis of the reaction mixture indicated that **3a** was quantitatively converted into **4a**. Similar treatment of **4a** did not result in reaction, even after being heated at reflux in benzene for 24 h.

Isomerization of 4 to 3: The general procedure for *N*-to-*C* isomerization is exemplified by the conversion of **4e** to **3e**: A solution of **4e** (0.00933 g, 0.0125 mmol) in benzene (10.0 mL) was heated at reflux for 24 h under an argon atmosphere. Evaporation of the solvent under reduced pressure gave a yellow residue. ^1H NMR (270 MHz, C_6D_6) spectroscopic analysis of the reaction mixture indicated that **4e** was quantitatively converted into **3e**. Similar treatment of **3e** did not result in reaction, even after being heated at reflux in benzene for 24 h. The conversion of **4k** in boiling benzene for 12 h gave a 51:49 diastereomeric pair of **3k** (99%, ^1H NMR spectroscopy with an internal standard), whereas no reaction took place upon heating a solution of **3k** in benzene. The conversion of **4l** in boiling benzene for 24 h gave a 52:48 diastereomeric pair of **3l** (75%, ^1H NMR spectroscopy with an internal standard).

General procedure for *C*-to-*N* interconversions from 3b or 4a with various phosphanes: A solution of **3b** (0.00933 g, 0.0125 mmol) or **4a** (0.0109 g, 0.0125 mmol), phosphane (monophosphane: 0.0500 mmol, diphosphane: 0.0250 mmol), and dibenzyl (0.0150 mmol) in benzene (10 mL) was heated under reflux for 24 h under an argon atmosphere. After removal of the solvent under reduced pressure, the residue underwent ^{1}H NMR (270 MHz, C_6D_6) spectroscopic analysis. Product yields were determined based on the internal standard (dibenzyl). Treating **3b** with dppb, dppf, and dcype gave **4g** (79%), **4h** (75%), and **4j** (71%) as the sole products, respectively, whereas similar treatment with PMe_2Ph, dppm, dppe, and dmpe afforded **3c** (94%), **3e** (80%), **3f** (81%), and **3i** (61%), respectively. Treating **4a** with $PMePh_2$, PMe_2Ph, dppm, dppe, and dmpe gave **3b** (85%), **3c** (79%), **3e** (51%), **3f** (72%), and **3i** (90%) as the sole product, respectively, whereas similar treatment with P(*i*Pr)$_3$, dppb, dppf, and dcype afforded **4d** (47%), **4g** (99%), **4h** (99%), and **4j** (99%).

Reaction of 4a with *t*BuNC: A solution of **4a** (0.436 g, 0.500 mmol) and *t*BuNC (0.166 g, 2.00 mmol) in benzene (40 mL) was heated at reflux for 24 h under an argon atmosphere. ^{1}H NMR spectroscopic analysis of the reaction mixture showed that **3k** was formed quantitatively. Removal of the solvent under reduced pressure and reprecipitation with hexane afforded **3k** (0.268 g, 39%) as a 52:48 diastereomeric mixture (^{1}H NMR spectroscopy).

Reaction of 6a with *t*BuNC: A solution of **6a** (0.401 g, 0.500 mmol) and *t*BuNC (0.166 g, 2.00 mmol) in benzene (40 mL) was heated at reflux for 24 h under an argon atmosphere. ^{1}H NMR spectroscopic analysis of the reaction mixture showed that [Ru{CH(CN)CO_2Et}(CN*t*Bu)(Cp)(PPh_3)] (**5k**) was formed in a quantitative yield. After removal of the solvent under reduced pressure, the residue underwent column chromatography (neutral alumina; eluent: acetone/hexane 1:4) to afford **5k** as a 62:38 diastereomeric mixture (0.223 g, 36%).

Preparation of 5k from 8: The reaction of **8** (0.547 g, 1.00 mmol) with Na[CH(CN)CO_2Et] (0.270 g, 2.00 mmol) was carried out in boiling ethanol (40 mL) for 24 h under an argon atmosphere. The mixture was concentrated under reduced pressure and reprecipitated with benzene to give **5k** as a yellow solid (0.527 g, 84%). ^{1}H NMR spectroscopic analysis of the Cp groups of **5k** showed that the d.r. is 70:30. ^{1}H NMR (500 MHz, C_6D_6): δ = 0.99 (t, J = 7.0 Hz, 3H; OCH_2CH_3 (minor)), 1.06 (s, 9H; C_4H_9 (major)), 1.09 (t, J = 7.0 Hz, 3H; OCH_2CH_3 (major)), 1.13 (s, 9H; C_4H_9 (minor)), 2.39 (d, J = 5.5 Hz, 1H; C*H*CN (major)), 2.66 (d, J = 5.5 Hz, 1H; C*H*CN (minor)), 3.84–4.16 (m, 2H; OCH_2CH_3), 4.68 (s, 5H; C_5H_5-(minor)), 4.77 (s, 5H; C_5H_5 (major)), 7.05–7.18 (m, 12H; Ar*H*), 7.55–7.62 (m, 6H; PC_6H_5 (*ortho*, minor)), 7.65–7.74 ppm (m, 6H; PC_6H_5 (*ortho*, major)); ^{31}P{^{1}H} NMR (202 MHz, C_6D_6): δ = 60.7 (s; major), 61.8 ppm (s; minor); IR (KBr) $\tilde{\nu}$ = 2197 (C≡N), 2112 (*t*BuNC), 1690 (CO), 1480, 1433, 1368, 1321, 1229 (CO), 1211, 1150, 1092, 1049, 806, 748, 696, 530 cm^{-1}; FABMS: m/z: 624 ([M]$^+$).

Preparation of (R^*_{Ru},S^*_C,R^*_{Ru},S^*_C)-15: A solution of **3a** (0.174 g, 0.200 mmol) in THF (0.5 mL) was allowed to stand at RT for 48 h. The resulting red precipitate was collected by filtration, washed with small portions of benzene, and dried under reduced pressure to give **15** as a yellow solid (0.0536 g, 22%). ^{1}H NMR spectroscopic analysis (500 MHz) of the reaction mixture showed that the reaction gave complex **15** as a single diastereomer. Similar treatment in [D_6]benzene afforded a 73:27 mixture of **15** and its minor diastereomer **16**. Minor diastereomer **16** was isolated by reprecipitation with benzene/hexane.

15: ^{1}H NMR (270 MHz, C_6D_6): δ = 2.95 (d, J = 5.0 Hz, 2H; C*H*CN), 4.75 (s, 10H; C_5H_5), 6.61–6.68 (m, 6H; Ar*H*), 6.94–7.10 (m, 18H; Ar*H*), 7.54–7.64 ppm (m, 16H; Ar*H*); ^{31}P{^{1}H} NMR (202 MHz, C_6D_6): δ = 57.2 ppm (s); IR (KBr) $\tilde{\nu}$ = 2195 (C≡N), 1479, 1431, 1300 (asym, S=O), 1143 (sym, S=O), 1091, 747, 691, 594, 532 cm^{-1}; FABMS: m/z: 1218 ([M]$^+$), 1038 ([M−NCCHSO$_2$Ph]$^+$), 691 ([M−2PPh$_3$]$^+$), 609 ([M−Ru(Cp)(NCCHSO$_2$Ph)(PPh$_3$)]$^+$).

16: ^{1}H NMR (270 MHz, C_6D_6): δ = 4.18 (d, J = 4.2 Hz, 1H), 4.22 (d, J = 4.2 Hz, 1H), 4.63 (s, 10H; C_5H_5), 7.05–7.30 (br m, 24H; Ar*H*), 7.68–7.80 ppm (br m, 16H; Ar*H*); FABMS: m/z: 1218 ([M]$^+$). The stereochemistry of **16** was tentatively assigned to be the unsymmetrical configuration of (R^*_{Ru},R^*_C,R^*_{Ru},S^*_C) or (R^*_{Ru},R^*_C,S^*_{Ru},R^*_C) from the low-field doublet of two nonequivalent α-protons of nitriles.

Ring-cleavage reactions of 15 with various ligands: A solution of **15** (0.0153 g, 0.0125 mmol) and phosphane (monophosphane: 0.0500 mmol, diphosphane: 0.0250 mmol) in benzene (10 mL) was heated at reflux overnight. After removal of the solvent under reduced pressure, the residue was analyzed by ^{1}H NMR spectroscopy (270 and 400 MHz, C_6D_6). Quantitative formation of **4a** and **4h** was observed when PPh_3 and dppf were used as ligands, whereas **3c** was formed quantitatively upon similar treatment with PMe_2Ph. Complex **3l** was obtained quantitatively (^{1}H NMR spectroscopy, (R^*_{Ru},S^*_C)/(R^*_{Ru},R^*_C) = 81:19) when the reaction was carried out in boiling benzene (10 mL) under CO (100 atm) for 24 h.

X-ray structure determination: Crystals suitable for X-ray diffraction were mounted on a glass fiber with epoxy adhesive. Intensity data were collected by using a Rigaku AFC-7R four-circle data collector with $Mo_{K\alpha}$ radiation (λ = 0.71069 nm). The unit cell parameters were determined by using a least-squares fit to 2θ values for 25 strong higher reflections. Three standard reflections were chosen and monitored every 150 reflections. Empirical absorption correction showed no significant decay during data collection. The structures of **3e**, **3k**, **3l**, **4a**, **4k**, **10**, and **15** were solved by direct or heavy-atom Patterson methods, and refined by the full-matrix least-squares method. In the subsequent refinement, the function $\Sigma\omega(|F_o|^2-|F_c|^2)^2$, in which F_o and F_c are the observed and calculated structure factor amplitudes, respectively, was minimized. The positions of all non-hydrogen atoms were determined from difference Fourier electron density maps and refined anisotropically. All calculations were performed by using the teXsan and Crystal Structure crystallographic software packages and illustrations were drawn by using ORTEP. The details of the structure determinations are given in Tables 2 and 3. CCDC 651717 (**3e**·$^1/_2CH_3COCH_3$), 651719 (**3k**), 651718 (**3l**·C_6H_6), 651720 (**4a**), 651721 (**4k**·C_6H_6), 651722 (**10**), and 652164 (**15**) contain the supplementary crystallographic data for this paper. These data can be obtained free of charge from The Cambridge Crystallographic Data Centre via www.ccdc.cam.ac.uk/data_request/cif.

Computational methods: All calculations were carried out by using the implementation of Becke's three-parameter hybrid functional by the Gaussian 03 program combined with the Lee–Yang–Parr correlation functional theory (B3LYP).[33, 34] We used the LANL2DZ basis set[35] that consists of the Dunning and Huzinaga valence double-z basis D95V for first-row atoms[36] and the Los Alamos effective core potential (ECP), which includes relativistic effects plus double-ζ atomic orbitals for ruthenium. Geometry optimizations were achieved by using analytical gradient techniques without any symmetry assumptions.[37] Stationary points were characterized by frequency calculations to verify that the transition-state structure has only one imaginary frequency. The intrinsic reaction coordinate path was traced to check the energy profiles that connect transition states with the two minima of the proposed mechanism by using a second-order integration method.[38] Zero-point energies and thermodynamic functions were computed for 298.15 K and 1 atm. The atomic charges of the optimized structures were calculated by using the NBO program bundled with the Gaussian 03 package.[39]

[1] a) [($Ph_3P)_2N$][Fe(CH_2CN)(CO)$_4$]: W. O. Siegl, J. P. Collman, *J. Am. Chem. Soc.* **1972**, *94*, 2516–2518; b) [Co(CHMeCN)-{ON=C(Me)C(Me)NOH}$_2$(Py)]: Y. Ohashi, Y. Tomotake, A. Uchida, Y. Sasada, *J. Am. Chem. Soc.* **1986**, *108*, 1196–1202; c) [Ni-(CH_2CN)$_2$(dppe)]: P. R. Alburquerque, A. R. Pinhas, J. A. K. Bauer, *Inorg. Chim. Acta* **2000**, *298*, 239–244; d) [PdAr{C(CN)R^{1}R^2}L$_2$]: D. A. Culkin, J. F. Hartwig, *J. Am. Chem. Soc.* **2002**, *124*, 9330–9331; e) [Cr(CH_2CN)(H_2O)$_5$]$^{2+}$: W. C. Kupferschmidt, R. B. Jordan, *J. Am. Chem. Soc.* **1984**, *106*, 991–995; f) [Ph$_4$P][Ir(CH_2CN)(CO)$_2$]: F. Porta, F. Ragaini, S. Cenini, F. Demartin, *Organometallics* **1990**, *9*, 929–935; g) [($Ph_3P)_2N$][Rh$_5$(CH_2CN)(CO)$_{14}$]: F. Ragaini, F. Porta, A. Fumagalli, F. Demartin, *Organometallics* **1991**, *10*, 3785–3789; h) [Ni(dippe)(CH_2CN)Cl]: T. A. Ateşin, T. Li, S. Lachaize, W. W. Brennessel, J. J. García, W. D. Jones, *J. Am. Chem. Soc.* **2007**, *129*, 7562–7569; i) [Ir(CH_2CN)(depe)$_2$H]Cl: A. D. English, T. Herskovitz,

J. Am. Chem. Soc. **1977**, *99*, 1648–1649; j) [Fe(CH_2CN)(dmpe)$_2$H]: S. D. Ittel, C. A. Tolman, A. D. English, J. P. Jesson, *J. Am. Chem. Soc.* **1978**, *100*, 7577–7585; k) [Pt{CH(CN)(CH_2NHPh)}(PEt_3)$_2$H]: R. L. Cowan, W. C. Trogler, *J. Am. Chem. Soc.* **1989**, *111*, 4750–4761; l) [Hg(CHRCN)X]: G. A. Russell, P. Chen, C.-F. Yao, B. H. Kim, *J. Am. Chem. Soc.* **1995**, *117*, 5967–5972.

[2] a) [Co[CH($CN)_2$](py)(salen)]: D. Cummins, B. M. Higson, E. D. McKenzie, *J. Chem. Soc. Dalton* **1973**, 414–419; b) [Pt{CH(CN)CO_2Me}(dppp)Me]: D. P. Arnold, M. A. Bennett, *J. Organomet. Chem.* **1980**, *199*, 119–135; c) [(Ph_3P)$_2$N][Au{CH($CN)_2$}$_2$]: J. Vicente, M.-T. Chicote, I. Saura-Llamas, M.-C. Lagunas, *J. Chem. Soc. Chem. Commun.* **1992**, 915–916; d) [Au{CH($CN)_2$}(PPh_3)]: S. Komiya, M. Iwata, T. Sone, A. Fukuoka, *J. Chem. Soc. Chem. Commun.* **1992**, 1109–1110; e) [$PdMe_2$-(NCCHCN)PyTp]: M. Kujime, S. Hikichi, M. Akita, *Organometallics* **2001**, *20*, 4049–4060.

[3] a) [XZnRCu(CH_2CN)]: P. Knochel, N. Jeong, M. J. Rozema, M. C. P. Yeh, *J. Am. Chem. Soc.* **1989**, *111*, 6474–6476; b) [Ce(CH_2CN)Cl_2]: H.-J. Liu, N. H. Al-said, *Tetrahedron Lett.* **1991**, *32*, 5473–5476; c) [Mn*t*BuCO_2(CH_2CN)]: M. T. Reetz, H. Haning, S. Stanchev, *Tetrahedron Lett.* **1992**, *33*, 6963–6966; d) [Fe(CH_2CN)Cl]: T. Kauffmann, H. Kieper, H. Pieper, *Chem. Ber.* **1992**, *125*, 899–905; e) [Ti-(CH_2CN)(*i*PrO)$_3$]: T. Kauffmann, H. Kieper, *Chem. Ber.* **1992**, *125*, 907–912; f) [Zn(CH_2CN)Cl]: M. R. Saidi, H. R. Khalaji, J. Ipaktschi, *J. Chem. Soc. Perkin Trans. 1* **1997**, 1983–1986.

[4] [Pd{CH(Et)CN}L_2]: a) F. Wu, S. R. Foley, C. T. Burns, R. F. Jordan, *J. Am. Chem. Soc.* **2005**, *127*, 1841–1853; b) F. Wu, R. F. Jordan, *Organometallics* **2006**, *25*, 5631–5637.

[5] a) [{Rh(CO)(PPh_3)$_2$}$_2$][NCC(CN)C(CN)C(CN)C(CN)CCN]: W. Beck, R. Schlodder, K. H. Lechler, *J. Organomet. Chem.* **1973**, *54*, 303–311; b) R. Schlodder, J. A. Ibers, *Inorg. Chem.* **1974**, *13*, 2870–2876; c) *trans*-[Pt(NCCHCO_2Me)(PEt_3)$_2$Ph]: reference [2b]; d) [Re(CO)$_5${NCC($CN)_2$}]: W. Sacher, U. Nagel, W. Beck, *Chem. Ber.* **1987**, *120*, 895–900; e) *trans*-[PtH{NCC(CN)C(CN)C($CN)_2$}-(PPh_3)$_2$]: L. Jäger, C. Tretner, H. Hartung, M. Biedermann, *Chem. Ber.* **1997**, *130*, 1007–1012; f) [PdAr(binap){NCC(CH_3)$_2$}]: reference [1d]; g) [Ir{NCC(CN)CH($CN)_2$}(PPh_3)$_2$(TCNE)]: J. S. Ricci, J. A. Ibers, *J. Am. Chem. Soc.* **1971**, *93*, 2391–2397; h) [Mo(dppe)$_2$N-(NCCHCOR)]: Y. Tanabe, H. Seino, Y. Ishii, M. Hidai, *J. Am. Chem. Soc.* **2000**, *122*, 1690–1699; i) reference [2e].

[6] Ru: a) [RuH(NCCHCO_2R)(NCCH_2CO_2R)(PPh_3)$_2$]: S. Komiya, Y. Mizuho, N. Kasuga, *Chem. Lett.* **1991**, 2127–2130; b) S.-I. Murahashi, T. Naota, H. Taki, M. Mizuno, H. Takaya, S. Komiya, Y. Mizuho, N. Oyasato, M. Hiraoka, M. Hirano, A. Fukuoka, *J. Am. Chem. Soc.* **1995**, *117*, 12436–12451; c) *trans*-[Ru(dppe)$_2$H-(NCCHCO_2R)]: M. Hirano, A. Takenaka, Y. Mizuho, M. Hiraoka, S. Komiya, *J. Chem. Soc. Dalton Trans.* **1999**, 3209–3216; d) [Ru(Cp)*(NCCHCO_2R)(PPh_3)$_2$]: S.-I. Murahashi, K. Take, T. Naota, H. Takaya, *Synlett* **2000**, 1016–1018; e) [Ru(Cp)(NCCHSO_2Ph)(PPh_3)$_2$]: T. Naota, A. Tannna, S.-I. Murahashi, *Chem. Commun.* **2001**, 63–64; Fe: f) [Fe(dppe)$_2$H-(NCCHCO_2R)] M. Hirano, S. Kiyota, M. Imoto, S. Komiya, *Chem. Commun.* **2000**, 1679–1680; Re: g) [Re(NCCH$^-$$CO_2$R)(NCC$H_2CO_2$R)($PMe_2Ph$)$_4$]: M. Hirano, M. Hirai, Y. Ito, T. Tsurumaki, A. Baba, A. Fukuoka, S. Komiya, *J. Organomet. Chem.* **1998**, *569*, 3–14.

[7] a) [Mn($MeOH)_2$(tcnq-tcnq)]$_n$: H. Zhao, R. A. Heintz, K. R. Dunbar, R. D. Rogers, *J. Am. Chem. Soc.* **1996**, *118*, 12844–12845; b) [Cu{C[C($CN)_2$]$_3$}($H_2O)_2$]$_n$: S. Triki, J. S. Pala, M. Decoster, P. Molinié, L. Toupet, *Angew. Chem.* **1999**, *111*, 155–158; *Angew. Chem. Int. Ed.* **1999**, *38*, 113–115; c) [MnTPP][C_3($CN)_5$]: M. L. Yates, A. M. Arif, J. L. Manson, B. A. Kalm, B. M. Burkhart, J. S. Miller, *Inorg. Chem.* **1998**, *37*, 840–841; d) (Me_4N)$_2$[Mn_4O_2-{NCC(NO)$CONH_2$}$_4$(MeCN)$_2$($H_2O)_6$](NO_3)$_4$·2H_2O: D. J. Price, S. R. Batten, K. J. Berry, B. Moubaraki, K. S. Murray, *Polyhedron* **2003**, *22*, 165–176.

[8] Pd: N. Tsukada, A. Shibuya, I. Nakamura, Y. Yamamoto, *J. Am. Chem. Soc.* **1997**, *119*, 8123–8124.

[9] Pd: M. M. Salter, V. Gevorgyan, S. Saito, Y. Yamamoto, *Chem. Commun.* **1996**, 17–18.

[10] Pd: Y. Yamamoto, M. Al-Masum, N. Asao, *J. Am. Chem. Soc.* **1994**, *116*, 6019–6020.

[11] Ru: a) T. Naota, H. Taki, M. Mizuno, S.-I. Murahashi, *J. Am. Chem. Soc.* **1989**, *111*, 5954–5955; b) H. Takaya, S.-I. Murahashi, *Synlett* **2001**, 991; c) N. Kumagai, S. Matsunaga, M. Shibasaki, *J. Am. Chem. Soc.* **2004**, *126*, 13632–13633; d) N. Kumagai, S. Matsunaga, M. Shibasaki, *Chem. Commun.* **2005**, 3600–3602; Pd: e) H. Nemoto, Y. Kubota, Y. Yamamoto, *J. Chem. Soc. Chem. Commun.* **1994**, 1665; Ir: f) Y. Lin, X. Zhu, M. Xiang, *J. Organomet. Chem.* **1993**, *448*, 215–218.

[12] Rh: Y. Yamamoto, Y. Kubota, Y. Honda, H. Fukui, N. Asao, H. Nemoto, *J. Am. Chem. Soc.* **1994**, *116*, 3161–3162.

[13] Ir: H. Takaya, T. Naota, S.-I. Murahashi, *J. Am. Chem. Soc.* **1998**, *120*, 4244–4245.

[14] Rh: a) S. Paganelli, A. Schionato, C. Botteghi, *Tetrahedron Lett.* **1991**, *32*, 2807–2810; b) M. Sawamura, H. Hamashima, Y. Ito, *J. Am. Chem. Soc.* **1992**, *114*, 8295–8296; c) M. Sawamura, H. Hamashima, Y. Ito, *Tetrahedron*, **1994**, *50*, 4439–4454; d) M. Sawamura, M. Sudoh, Y. Ito, *J. Am. Chem. Soc.* **1996**, *118*, 3309–3310; e) M. Sawamura, H. Hamashima, Y. Ito, *Bull. Chem. Soc. Jpn.* **2000**, *73*, 2559–2562; f) Y. Motoyama, Y. Koga, K. Kobayashi, K. Aoki, H. Nishiyama, *Chem. Eur. J.* **2002**, *8*, 2968–2975; Ir: g) Z. Hou, T. Koizumi, A. Fujita, H. Yamazaki, Y. Wakatsuki, *J. Am. Chem. Soc.* **2001**, *123*, 5812–5813; h) H. Takaya, K. Yoshida, H. Terai, K. Isozaki, S.-I. Murahashi, *Angew. Chem.* **2003**, *115*, 3424–3426; *Angew. Chem. Int. Ed.* **2003**, *42*, 3302–3304, ; i) D. Carmona, J. Ferrer, M. Lorenzo, F. J. Lahoz, I. T. Dobrinovitch, L. A. Oro, *Eur. J. Inorg. Chem.* **2005**, *9*, 1657–1664.

[15] a) J. J. Doney, R. G. Bergman, C. H. Heathcock, *J. Am. Chem. Soc.* **1985**, *107*, 3724–3726; b) G. A. Slough, R. G. Bergman, C. H. Heathcock, *J. Am. Chem. Soc.* **1989**, *111*, 938–949; c) J. G. Stack, J. J. Doney, R. G. Bergman, C. H. Heathcock, *Organometallics* **1990**, *9*, 453–466; d) J. F. Hartwig, R. G. Bergman, R. A. Andersen, *J. Am. Chem. Soc.* **1990**, *112*, 3234–3236; e) J. F. Hartwig, R. A. Andersen, R. G. Bergman, *J. Am. Chem. Soc.* **1990**, *112*, 5670–5671; f) J. G. Stack, R. D. Simpson, F. J. Hollander, R. G. Bergman, C. H. Heathcock, *J. Am. Chem. Soc.* **1990**, *112*, 2716–2729; g) J. R. Fulton, M. W. Bouwkamp, R. G. Bergman, *J. Am. Chem. Soc.* **2000**, *122*, 8799–8800.

[16] Catalytic reactions: a) E. Gómez-Bengoa, J. M. Cuerva, C. Mateo, A. M. Echavarren, *J. Am. Chem. Soc.* **1996**, *118*, 8553–8565; b) H. Gröger, E. M. Vogl, M. Shibasaki, *Chem. Eur. J.* **1998**, *4*, 1137–1141; c) B. M. Trost, F. D. Toste, A. B. Pinkerton, *Chem. Rev.* **2001**, *101*, 2067–2096; d) M. Shibasaki, N. Yoshikawa, *Chem. Rev.* **2002**, *102*, 2187–2209; e) K. Mikami, M. Terada, H. Matsuzawa, *Angew. Chem.* **2002**, *114*, 3704–3722; *Angew. Chem. Int. Ed.* **2002**, *41*, 3554–3571; f) R. R. Huddlerston, M. J. Krische, *Synlett* **2003**, 12–21; g) H.-Y. Jang, M. J. Krische, *Acc. Chem. Res.* **2004**, *37*, 653–661; h) Y. Hamashima, M. Sodeoka, *Chem. Rec.* **2004**, *4*, 231–242; i) M. Sodeoka, Y. Hamashima, *Y. Bull. Chem. Soc. Jpn.* **2005**, *78*, 941–956; j) T. Ikariya, K. Murata, R. Noyori, *Org. Biomol. Chem.* **2006**, *4*, 393–406.

[17] T. Naota, A. Tannna, S.-I. Murahashi, *J. Am. Chem. Soc.* **2000**, *122*, 2960–2961.

[18] T. Naota, A. Tannna, S. Kamuro, S.-I. Murahashi, *J. Am. Chem. Soc.* **2002**, *124*, 6842–6843.

[19] V. Y. Lee, H. Ranaivonjatovo, J. Escudié, J. Satgé, A. Dubourg, J.-P. Declercq, M. P. Egorov, O. M. Nefedov, *Organometallics* **1998**, *17*, 1517–1522.

[20] C. A. Tolman, *Chem. Rev.* **1977**, *77*, 313–348.

[21] K. S. MacFarlane, A. M. Joshi, S. J. Rettig, B. R. James, *Inorg. Chem.* **1996**, *35*, 7304–7310.

[22] I.-Y. Wu, J. T. Lin, J. Luo, S.-S. Sun, C.-S. Li, K. J. Lin, C. Tsai, C.-C. Hsu, J.-L. Lin, *Organometallics* **1997**, *16*, 2038–2048.

[23] a) B. E. Mann, A. Musco, *J. Chem. Soc. Dalton Trans.* **1980**, 776–785; b) M. S. Sanford, J. A. Love, R. H. Grubbs, *J. Am. Chem. Soc.* **2001**, *123*, 6543–6554.

[24] M. I. Bruce, R. C. Wallis, *Aust. J. Chem.* **1981**, *34*, 209–213.

[25] a) R. J. Balahura, N. A. Lewis, *Coord. Chem. Rev.* **1976**, 20, 109–153; b) F. A. Cotton, G. Wilkinson, *Advanced Inorganic Chemistry*, 5th Ed., Wiley, New York, **1988**, p. 38; c) C. S. Slone, D. A. Weinberger in *Progress in Inorganic Chemistry*; (Ed.: K. D. Karlin), Wiley, New York, **1999**, pp. 233–350; d) Y. Yamanoi, T. Imamoto, *Reviews on Heteroatom Chemistry* **1999**, 20, 227–248; e) V. Y. Kukushkin, A. J. L. Pombeiro, *Chem. Rev.* **2002**, *102*, 1771–1802; f) P. Coppens, I. Novozhilova, A. Kovalevsky, *Chem. Rev.* **2002**, *102*, 861–883; g) W. D. Harman, *Coord. Chem. Rev.* **2004**, *248*, 853–866.

[26] a) L. Cheng, I. Novozhilova, C. Kim, A. Kovalevsky, K. A. Bagley, P. Coppens, G. B. Richter-Addo, *J. Am. Chem. Soc.* **2000**, *122*, 7142–7143; b) J. Lee, A. Y. Kovalevsky, I. V. Novozhilova, K. A. Bagley, P. Coppens, G. B. Richter-Addo, *J. Am. Chem. Soc.* **2004**, *126*, 7180–7181; c) I. V. Novozhilova, P. Coppens, J. Lee, G. B. Richter-Addo, K. A. Bagley, *J. Am. Chem. Soc.* **2006**, *128*, 2093–2104.

[27] a) W. G. Jackson, G. A. Lawrence, P. A. Ley, A. M. Sargeson, *J. Chem. Soc. Chem. Commun.* **1982**, 70–72; b) K. Miyoshi, N. Katoda, H. Yoneda, *Inorg. Chem.* **1983**, *22*, 1839–1843; c) S. Balt, H. J. A. M. Kuipers, W. E. Renkema, *J. Chem. Soc. Dalton Trans.* **1983**, 1739–1741.

[28] a) A. Yeh, N. Scott, H. Taube, *Inorg. Chem.* **1982**, *21*, 2542–2545; b) M. Mares, D. A. Palmer, H. Kelm, *Inorg. Chim. Acta* **1982**, *60*, 123–127; c) A. Y. Kovalevsky, K. A. Bagley, P. Coppens, *J. Am. Chem. Soc.* **2002**, *124*, 9241–9248.

[29] P. M. Angus, W. G. Jackson, *Inorg. Chem.* **1991**, *30*, 4806–4813.

[30] a) R. H. Fish, *J. Am. Chem. Soc.* **1974**, *96*, 6664–6669; b) S. Baba, T. Ogura, S. Kawaguchi, *Bull. Chem. Soc. Jpn.* **1974**, *47*, 665–668; c) S. Komiya, J. K. Kochi, *J. Am. Chem. Soc.* **1977**, *99*, 3695–3704; d) S. Kiyota, J. Tamuki, N. Komine, M. Hirano, S. Komiya, *Chem. Lett.* **2005**, *34*, 498–499; e) references [15a–c, e].

[31] a) D. Lucas, Z. Modarres-Tehrani, Y. Mugnier, A. Antinolo, I. Del Hierro, A. Otero, F. Fajardo, *New J. Chem.* **1996**, *20*, 385–391; b) S. Sakaki, B. Biswas, M. Sugimoto, *Organometallics* **1998**, *17*, 1278–1289; c) M. Etienne, C. Carfagna, P. Lorente, R. Mathieu, D. de Montauzon, *Organometallics* **1999**, *18*, 3075–3086; d) F. L. Taw, P. S. White, R. G. Bergman, M. Brookhart, *J. Am. Chem. Soc.* **2002**, *124*, 4192–4193; e) J. J. García, A. Arévalo, N. M. Brunkan, W. D. Jones, *Organometallics* **2004**, *23*, 3997–4002.

[32] J. Ruiz, V. Rodríguez, G. López, J. Casabó, E. Molins, C. Miravitlles, *Organometallics* **1999**, *18*, 1177–1184.

[33] Gaussian 03, revision C.02, M. J. Frisch, G. W. Trucks, H. B. Schlegel, G. E. Scuseria, M. A. Robb, J. R. Cheeseman, J. A. Montgomery, Jr., T. Vreven, K. N. Kudin, J. C. Burant, J. M. Millam, S. S. Iyengar, J. Tomasi, V. Barone, B. Mennucci, M. Cossi, G. Scalmani, N. Rega, G. A. Petersson, H. Nakatsuji, M. Hada, M. Ehara, K. Toyota, R. Fukuda, J. Hasegawa, M. Ishida, T. Nakajima, Y. Honda, O. Kitao, H. Nakai, M. Klene, X. Li, J. E. Knox, H. P. Hratchian, J. B. Cross, V. Bakken, C. Adamo, J. Jaramillo, R. Gomperts, R. E. Stratmann, O. Yazyev, A. J. Austin, R. Cammi, C. Pomelli, J. W. Ochterski, P. Y. Ayala, K. Morokuma, G. A. Voth, P. Salvador, J. J. Dannenberg, V. G. Zakrzewski, S. Dapprich, A. D. Daniels, M. C. Strain, O. Farkas, D. K. Malick, A. D. Rabuck, K. Raghavachari, J. B. Foresman, J. V. Ortiz, Q. Cui, A. G. Baboul, S. Clifford, J. Cioslowski, B. B. Stefanov, G. Liu, A. Liashenko, P. Piskorz, I. Komaromi, R. L. Martin, D. J. Fox, T. Keith, M. A. Al-Laham, C. Y. Peng, A. Nanayakkara, M. Challacombe, P. M. W. Gill, B. Johnson, W. Chen, M. W. Wong, C. Gonzalez, J. A. Pople, Gaussian, Inc., Wallingford CT, **2004**.

[34] a) A. D. Becke, *J. Chem. Phys.* **1993**, *98*, 1372–1377; b) A. D. Becke, *J. Chem. Phys.* **1993**, *98*, 5648–5652.

[35] P. J. Hay, W. R. Wadt, *J. Chem. Phys.* **1985**, *82*, 270–283.

[36] T. H. Dunning, Jr., P. J. Hay in *Modern Theoretical Chemistry, Vol. 3* (Ed.: H. F. Schaefer III), Plenum, New York, **1977**, pp. 1–28.

[37] H. B. Schlegel in *Modern Electronic Structure Theory* (Ed.: D. R. Yarkony), World Scientific, Singapore, **1995**, pp. 459–500.

[38] a) C. Gonzalez, H. B. Schlegel, *J. Phys. Chem.* **1990**, *94*, 5523–5527; b) C. Gonzalez, H. B. Schlegel, *J. Chem. Phys.* **1991**, *95*, 5853–5860.

[39] A. E. Reed, L. A. Curtiss, F. Weinhold, *Chem. Rev.* **1988**, *88*, 899–926.

Received: August 24, 2007
Published online: January 14, 2008

